Separation & Purification Reviews
Publication details, including instructions for authors and subscription information:
http://www.informaworld.com/smpp/title~content=t713597294

Separation of Cations by Foam and Bubble Fractionation

E. Valdes-Krieg; C. J. King; H. H. Sephton

To cite this Article Valdes-Krieg, E. , King, C. J. and Sephton, H. H.(1977) 'Separation of Cations by Foam and Bubble Fractionation', Separation & Purification Reviews, 6: 2, 221 — 285
To link to this Article: DOI: 10.1080/15422117708544704
URL: http://dx.doi.org/10.1080/15422117708544704

SEPARATION AND PURIFICATION METHODS, 6(2), 221-285 (1977)

SEPARATION OF CATIONS BY FOAM AND BUBBLE FRACTIONATION

E. Valdes-Krieg, C.J. King & H.H. Sephton
Department of Chemical Engineering and
Sea Water Conversion Laboratory,
University of California, Berkeley, California 94720

ABSTRACT

A comparison is made of separation techniques based upon surface activity in foam and/or bubble contactors. Factors involved in separation by foam and bubble fractionation are evaluated, especially those governing capacity and selectivity for removal of metallic counter-ions. Experimental results are presented for the removal of copper, cobalt and nickel. Methods of measuring surface equilibria are outlined, and results for metal-ion systems are analyzed in terms of diffuse-double-layer and mass-action theories.

Mathematical models are presented for the analysis of combined bubble and foam fractionation. An analytical solution is obtained for the case of infinitely rapid mass transfer and linear surface equilibrium, and is extended through a graphical approach suitable for general, non-linear equilibria. A design improvement for enhanced removal of counter-ion species involves

adding surfactant to a point in a bubble column well below the main feed containing the species to be separated.

INTRODUCTION

Removal of pollutants and valuable solutes present in water in small quantities is becoming more and more important. Continued and increasing demands for certain minerals call for recoveries from more dilute liquors as traditional sources diminish or become insufficient. Increased concern for potential toxicity of certain elements in water[1], even if present in minute amounts, makes it necessary to develop efficient processes for removing them.

Processes for removing ions from water when present in small amounts include precipitation and settling, ion exchange, liquid extraction, electrodeposition and adsorptive bubble separation processes, among the most viable. This study focusses on the latter process as a promising alternative for this separation problem.

Removal and/or recovery of ions by adsorptive bubble separation processes has been dealt with extensively. The review by Rubin and Gaden[2] covers work up to that year. More recent reviews include those by Lemlich[3,4], Somasundaran[5], and Grieves[6].

Adsorptive Bubble Separation Processes

Adsorptive bubble separation processes are among the less common separation processes developed in recent years. These processes have been found effective for the removal of a wide variety of solutes and particulate matter from water, particularly when present in very low concentrations. Mineral flotation, which has been used successfully for many years, falls in this category.

As in all separation processes, advantage is taken of a distinct property of the system in question to effect separation; this property is the tendency of certain solutes (surfactants) to accumulate at air-liquid and solid-liquid interfaces.

Several types of surfactants can interact with non-surfactive solutes or particles, enabling one to accumulate such solutes or solids at bubble-liquid interfaces. Accumulation is achieved through interactions between the species of interest and surfactant adsorbed at a gas-liquid interface, in the case of solutes. Surfactant-ion interactions include ion-ion interactions, e.g., long-chain sulfates or sulfonates with cations; formation of a compound with little dissociation, e.g., long-chain sulfates with calcium at high concentration; chelation, e.g., long-chain acids with transition-series cations; and covalent bonding with organic compounds.

Karger, et al.[7] have proposed a terminology to classify the various processes resulting from various accumulation mechanisms at air-liquid interfaces. Processes in which surfactant addition to aqueous solutions gives rise to stable foams upon sparging of gas bubbles are classified as follows:

Foam Fractionation: Soluble species that are surfactive themselves or can interact with a surfactive solute are collected at bubble interfaces. Bubbles then generate a stable foam that conveys the enriched solution surrounding them out of a contactor. At the same time, excess liquid is drained from in between the bubbles. Collapsed foam (foamate) consists mainly of liquid that formed thin layers around the foam bubbles, which is rich in the species that were preferentially adsorbed or coadsorbed at gas-liquid interfaces.

Theoretically one can achieve substantial enrichment of solutes of interest in foams, given the large portion of bubble interfaces occupied by surfactants and coadsorbed species. In practice such enrichments are not realizable because of slow liquid drainage in foams[8-10], and the necessity of having a layer of finite thickness surrounding each bubble in order to impart it stability[11]. The process of enrichment in the simplest contactor (fig. 1a) can be visualized as equilibration of solution with a given interfacial area throughput (flow of bubbles of known dimensions). Once the bubbles leave the liquid pool in the form of foam, a volume of liquid remains entrained in it. The less the amount of entrained liquid, the greater the fraction of collected species and the greater the enrichment.

The entrainment phenomena described above have led to some confusion. Increasing enrichments can be obtained by allowing the foam to drain longer before collapsing it at constant operation conditions, i.e., using constant flows of gas and liquid and attaining the same equilibrium surface enrichment. The degree of enrichment of the foam is a function of the amount of liquid allowed to drain from the foam.

Separations of surfactants and non-surfactive species using foam fractionation in multistage modes have been studied using various feed and reflux arrangements[12-16]. Some of these arrangements are shown in fig. 1b-e.

The distinct characteristic of this process when applied to the removal of non-surfactive solutes is the potential stoichiometric relation of surfactant removed to total non-surfactive species removed. With exceptions attributable to other mechanisms (e.g., precipitation), foam separation results in amounts of non-surfac-

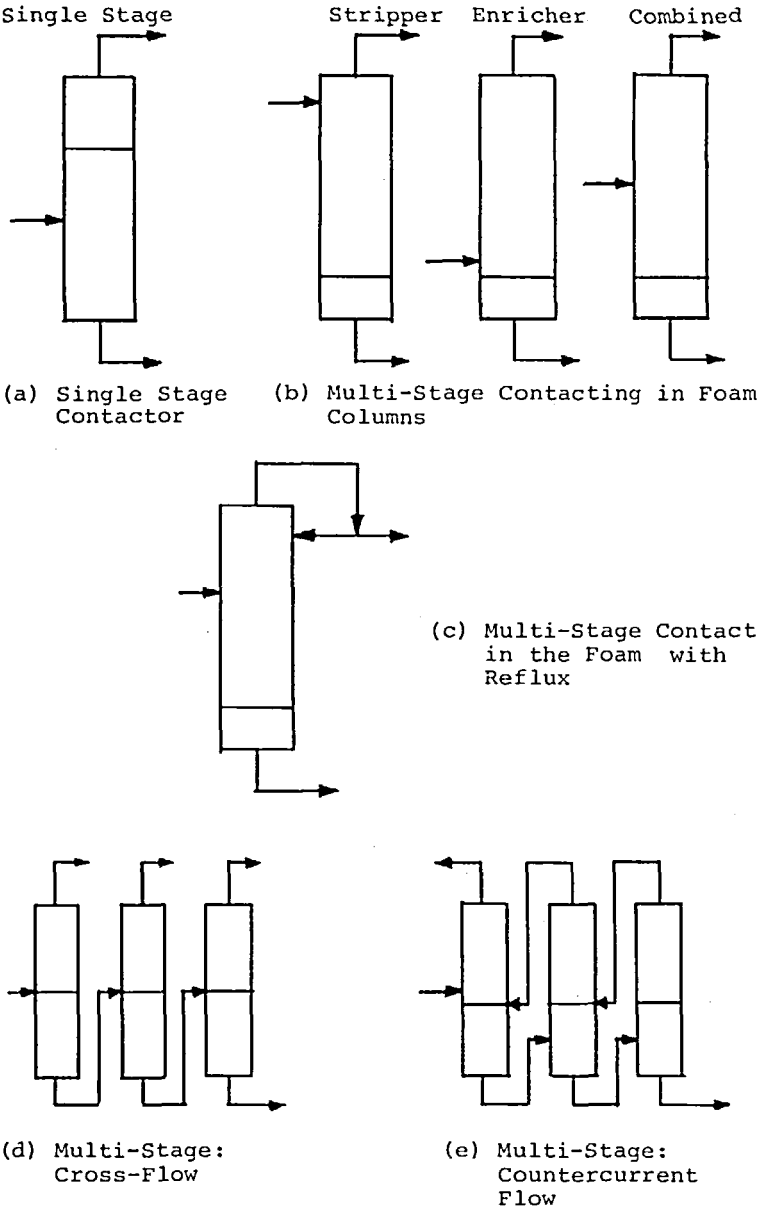

FIGURE 1

Foam fractionation schemes.

tive species removed that cannot exceed stoichiometric matching with the surfactant at gas-bubble surfaces.

Ion and Molecular Flotation: The removal of non-surfactive species in ion and molecular flotation occurs via insoluble or sparingly soluble compounds formed between the solute in question and the surfactant used to effect the separation[17,18].

When a surfactant can be found that yields a low-dissociation compound with the ion or molecule of interest, this technique offers an advantage in the relatively high selectivities attainable. Most of these systems exhibit formation of a scum upon sparging, rather than a foam. Separation efficiency is in most cases limited by redispersion of the scum layer in the contactor. This process is also potentially stoichiometric, i.e., the solute removed is at most stoichiometrically equivalent to the surfactant removed.

Flotation: This is the oldest of adsorptive bubble separation processes, and has been mostly applied to the flotation of minerals[19-21]. This process utilizes adsorption of a surfactive solute on a solid surface to render it hydrophobic and thus floatable by air bubbles. In this process the amount of solids separated is usually much greater than stoichiometric to the amount of surfactant used. A small coverage of particle surfaces with surfactant is enough to render particles floatable.

A relatively new approach for removal of ions in solution is precipitate flotation. This process consists of precipitating an ion of interest, followed by removal of the precipitate through flotation. The precipitation can occur with high selectivity over competing species. An amount of surfactant lower than

that required for equivalent separation of soluble species is used. The process has been carried out by precipitating hydroxides through a pH change[22,23] and by precipitating sulfides[24,etc.]. Its application is limited to ions that can form sufficiently insoluble precipitates at low concentrations without an excessive amount of precipitant and in the absence of ions that may form undesirable precipitates. The feasibility of this approach is also dependent on nucleation rates, strength of attachment on bubbles, and foam stability. The latter two factors affect redispersion and all three affect separation efficiency.

The use of flocculants in precipitate flotation[25] is an innovation towards more efficient separation using this process. The same is true for processes that generate a precipitate or add solid matter that can adsorb or exchange ions (e.g., adsorbing colloid flotation). The solid phase is subsequently removed by flotation[26].

Non-foaming Processes: These processes differ from foam fractionation or flotation as defined above in that the surfactant or the operating conditions used do not afford a stable foam. In such cases coalescence of bubbles at the liquid-pool surface brings about an enrichment of surfactive materials in that region, accompanied by depletion of lower regions in the pool[27-30]. Mixing due to flow of air bubbles tends to reduce the enrichment in the upper layers of liquid. This phenomenon has so far limited the applicability of this approach.

COLLECTORS FOR ION REMOVAL

Ionic surfactants are the most widely used for removal of cations and anions from solution. Some

studies have been made to determine the applicability of chelating surfactants, composed of a chelating group (preferentially ionizable) attached to a long aliphatic chain[15,31].

Selection of a surfactant to be used for ion removal is the first step towards a successful separation process. For purposes of the process, only the portion of surfactant adsorbed at bubble interfaces is useful to effect the separation. Surfactant remaining in solution or in micelle form after the gas bubbles and solution are contacted constitutes a loss in removal capacity, a loss of surfactant, and/or contamination that has to be removed subsequently. The following is a simplified analysis to examine the important factors to be taken into account when selecting a surfactant for a given application:

Surface Activity

Adsorption of surfactants at air-liquid interfaces results from exclusion of the organic portion of the molecule from bulk solution. The well-known Gibbs adsorption isotherm makes use of the fact that system free energy is lowered as the surface tension of the system is lowered, or, equivalently, as a solute showing little interaction with solvent molecules enriches a gas-liquid interface[32].

An extension of the Gibbs isotherm to account for the presence of ionic species in solution was developed by Davies and Rideal[33]. It assumes that the adsorbed layer is a "phase" of liquid whose volume is given by a depth, δ (cm), and unit surface area (cm^2). This phase is called subsurface "s". The other phase to be considered is the bulk liquid, or phase "b". For thermodynamic equilibrium the chemical potentials (μ) of phases b and s must be equal:

$$\mu_s = \mu_b \quad (1)$$

or

$$\mu_s^o + RT \ln a_s = \mu_b^o + RT \ln a_b \quad (2)$$

where μ_s^o and μ_b^o refer to standard potentials for phases s and b, respectively, and a_b and a_s indicate activities, expressed per unit volume. Rearranging, one obtains:

$$a_s = a_b \exp[(\mu_b^o - \mu_s^o)/RT] \quad (3)$$

Introducing activity coefficients (γ) and concentrations (c) for both phases, defining the term ($\mu_s^o - \mu_b^o$) as λ (standard free energy of desorption), and noting that surface activity per unit area, Γ, is given by $\gamma c_s \delta$, we obtain:

$$\Gamma = (\gamma_b/\gamma_s)\delta c_b \exp(\lambda/RT) \quad (4)$$

The familiar form of the Gibbs isotherm is given as a function of surface tension, σ (dynes/cm), as:

$$\Gamma = -\frac{\gamma_b c_b}{RT} \frac{\partial \sigma}{\partial (\gamma_b c_b)} \quad (5)$$

Both equations enable one to obtain surface concentration (Γ) and free energy of desorption (λ) estimates from surface-tension data. Equation 4 gives a simple way of relating surfactant behavior to molecular parameters. Limitations of this model are the difficulty of predicting activity coefficients in ionic solution and the assumption of a constant free energy of desorption. Keeping in mind these limitations, one can visualize the effects of different molecular and solution parameters on surfactant performance.

For qualitative purposes, the effects of ionic group and length of organic radical can be assumed additive in the free energy of desorption term (λ) defined above. A free energy term per methylene group in an aliphatic chain (w), a term accounting for polarity (λ_p) and a term accounting for electrostatic repulsion ($z_s e \psi_o$) add to give the standard free energy of desorption[33]. For

an ionic surfactant with a carbon number, n, in an aliphatic chain, λ is given by:

$$\lambda = nw + \lambda_p - z_s e\psi_o \quad (6)$$

The electrostatic repulsion term is the product of surfactant valence, z_s (assuming it is completely ionized), electron charge, e, and surface potential ψ_o, given as a function of surface concentration.

Using experimental values for w and estimates for δ based on molecular dimensions[34], equation 3 can be used to estimate surface concentrations and distribution coefficients for several ionic surfactant homologs. Figure 2 shows results for alkyl sulfate homologs at a constant bulk-liquid concentration of 50 parts per million (ppm) by weight. These calculations, as well as experimental data, indicate increased surface activity with increasing chain length.

Solubility and Cricital Micelle Concentration

Surfactant solubility and critical micelle concentration are temperature-dependent specific properties for surfactants. Criticial micelle concentration (CMC) is the concentration beyond which surfactant molecules or ions agglomerate into n-mers called micelles[35,36], without significant further enrichment at gas-liquid interfaces.

Figure 3 shows solubility and CMC data for the homologous series of alkyl sulfonates[34,37]. The plot indicates the concentration range below the critical micelle concentration for each homolog, which in all cases is lower than the solubility. Comparison of figs. 2 and 3 also reveals that high molecular weight surfactants can reach significant surface enrichments at low bulk-liquid concentrations, well below the CMC, resulting in potentially better recoveries in foam and

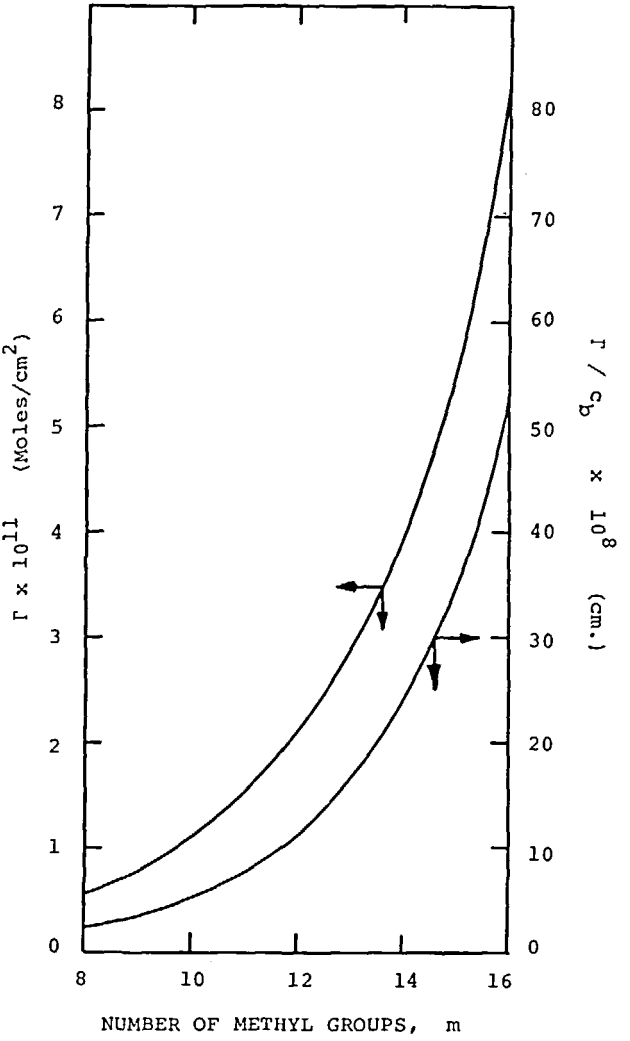

FIGURE 2
Influence of molecular weight on surfactant adsorption and distribution coefficients for solutions with constant weight concentration of surfactant (50 ppm).

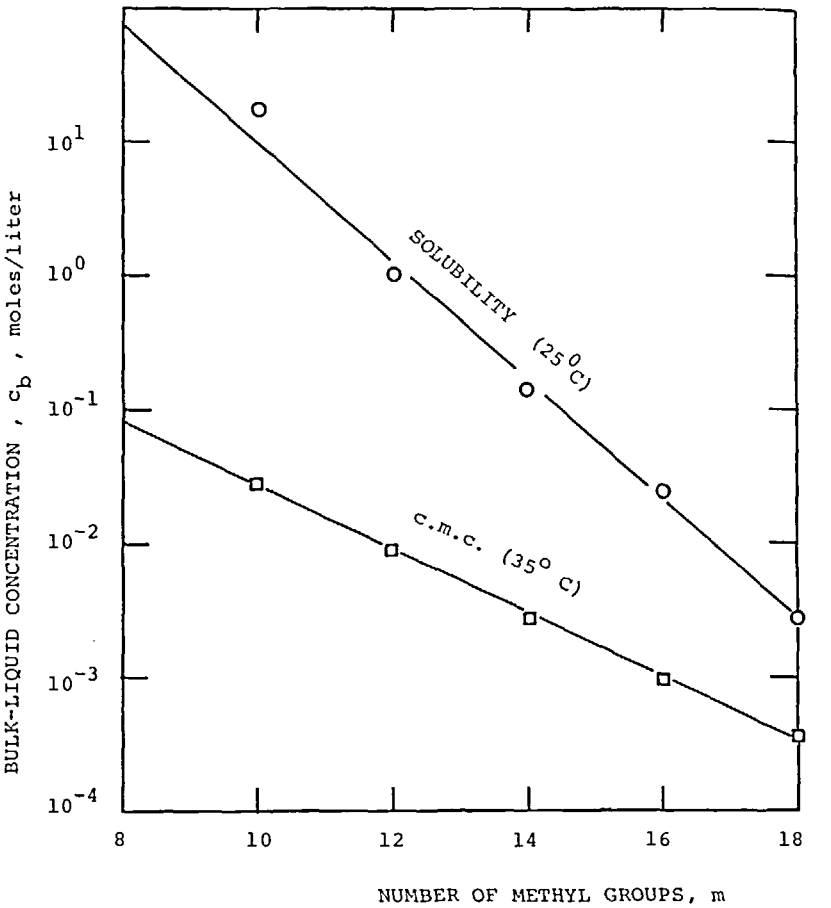

FIGURE 3
Solubility and critical micelle concentration of N-alkyl sulfonates.

bubble fractionation processes because of their higher distribution coefficients.

Dissociation

The idealized analysis used to describe the influence of molecular and ionic factors on surfactant adsorption shows a marked effect of ionic charge on the surface enrichments attainable. Shorter-chain

surfactants show a hydrophobic-hydrophilic balance that favors the liquid phase over adsorption at gas-liquid interfaces. Implied in the assumptions used is the postulate that adsorbed surfactants are completely ionized (strong acid or base behavior). Application of ABS processes to solutions of ions that form sparingly soluble surfactant compounds invalidates this assumption. Calculations using this simplified model[38], show that surfactant distribution coefficients (Γ/c) at a constant bulk-liquid concentration (50 ppm) can increase from two to six times for 50% as opposed to 100% dissociation in sulfates with eight to fourteen methylene groups, respectively.

Temperature Effects

Temperature effects on surfactant adsorption have been described using the isobaric rate of change of the standard free energy of desorption (λ) with temperature, giving the entropy of desorption:

$$\left(\frac{\partial \lambda}{\partial T}\right)_p = -\Delta S_d \qquad (7)$$

Observed values, derived from surface tension measurements[39], indicate entropy losses upon desorption for long-chain species, and the opposite effect for shorter-chain surfactants. One possible reason for this behavior is the tendency of long-chain species to coil up in solution, thereby diminishing the number of degrees of freedom as compared to a "stretched" ion or molecule at the interface. This indicates that adsorption should be enhanced at higher temperatures, as has been confirmed in practice[40,41].

Foam Stability

Foam stability can only indirectly be related to adsorption density. It has more to do with other factors such as surface viscosity, drainage rates and surfactant

purity. There is at present no a priori method of establishing whether a given molecule or ion will produce a stable foam when air is sparged into a solution. Quantitative tests of foam stability[11] are not reproducible to a reasonable degree of accuracy, nor are they easily related to actual operation of a contactor; therefore pilot-scale tests are necessary to carry out a selection between potential surfactants for a given process on the basis of foam stability. Of course, the surfactant used for foam stabilization may be different from that used for ion collection.

Collector Selection

In selecting a collector for a given application the following criteria can be applied:

a) The surfactant to be used should have the highest molecular weight allowed by a reasonable CMC. In most cases the additional weight of surfactant added per mole as separating agent will be more than offset by the higher distribution coefficients obtained and thus higher recoveries attainable.

b) An ionic surfactant with polar groups in its alkyl chain will tend to adsorb more readily. This can be inferred from the molecular parameters that add up to a calculated free energy of desorption (equation 6). Polar groups within an organic chain can in some cases lead to reduced repulsion between ionic groups at the interface and thus to enhanced adsorption.

c) A surfactant that forms strong bonds with the ion to be collected will exhibit both higher selectivity for the ion in question and increased adsorption, due to reduced electrostatic repulsion at the gas-liquid interface.

Somasundaran[5] and Lemlich[4] cover available information on ions separated with various surfactants.

DETERMINATION OF SURFACTANT EQUILIBRIA

As described above, calculation of surface equilibrium from surface tension data is limited by the number of assumptions made in the mathematical treatment used and by the number of fitted constants and variables necessary to utilize a model taking more factors into account.

Direct equilibrium measurements have been made using radioactive-labelled surfactants and radiotracer techniques[42,43]. These measurements disagree in some ways with surface equilibria calculated from surface tension data.

Direct foaming has been used to measure surface equilibria[44]. The present authors[45] have compared the latter method with a method that measures liquid depletion during cocurrent flow instead of foam enrichment to compute surface equilibria. The two methods are described in more detail below, in connection with ion-removal equilibria.

SURFACTANT MASS TRANSFER

Contact times necessary for a close approach to equilibrium in surfactant adsorption determine the contactor length necessary for efficient separation. The fact that swarms of bubbles generate significant agitation has in some cases led authors to conclude that surfactant adsorption is infinitely fast.

Radiotracer studies of rates of surfactant adsorption on quiescent surfaces[43] indicate that an adsorption barrier slows surfactant adsorption at high surface densities. Measurements carried out in a cocurrent column for bubble-liquid contact[38] also point to such a

barrier. Experiments at low surfactant concentration showed diffusional effects predominating. Under these conditions an overall mass transfer coefficient, K_x, based on diffusional limitations in the liquid phase and derived from concentration profiles, gave coefficients of the same order of magnitude as those obtained for liquid-phase-controlled gas-liquid mass transfer in a bubble column[46]. Experiments at high surfactant concentrations indicated near constancy of an overall mass transfer coefficient based on the surface phase ($K_y a$). This coefficient was dependent on ionic strength, as would be expected from increased electrostatic repulsion at the interface for low-ionic-strength systems.

Foaming contactors are mass-transfer limited in the liquid pool, with a height of transfer unit (HTU) of 10 to 30 cm, for typical operation conditions[45]. Measurement of mass-transfer rates in the foam portion of a foaming contactor resulted in HTU values down to about 1 cm[9].

REMOVAL OF METAL IONS USING ABS PROCESSES

Attachment of ions to charged interfaces led Walling and coworkers[47] to try their removal by sparging gas in an ionic-surfactant solution. Many application studies have been made since then; Lemlich[4] and Grieves[6] reviewed the literature in this field. Compared with the amount of effort devoted to finding new applications for this process, relatively few studies have concentrated upon important basic principles governing the separation.

In order to apply ABS processes successfully, two basic parameters must be understood. There parameters are:

a) Adsorption capacity of surfactant-loaded interfaces.

b) Selectivity among ions for sorption at interfaces.

The first parameter is primarily affected by surfactant enrichment per unit interfacial area. The second parameter is dependent upon the nature of the surfactant used, the nature and concentration of the ion or ions of interest, and the amount and nature of competing species in solution.

A description of how ion enrichment is measured and of what factors favor or diminish enrichment follows, along with an attempt to rationalize some of the governing mechanisms.

Measurement of Ion Enrichment

Surface concentrations of non-surfactive counter-ions interacting with adsorbed surfactant can be measured by experiments similar to the ones used to measure surfactant equilibria. An exception is the radiotracer technique, which enables one to measure adsorption of only non-surfactive ions or surfactants separately.

A foaming experiment can be carried out by contacting a given amount of solution with an amount of gas of known bubble diameter. This is done in a vessel that ensures sufficient approach to equilibrium. Experiments should be run with a continuous throughput of solution and gas to ensure steady-state operation. Given volumetric throughputs of liquid and gas, L and G, respectively, with a surface-area averaged bubble diameter, d, and a fraction, f, of the liquid entering the contactor being carried over in the foam, a mass balance gives the surface concentration (Γ) for the species of interest. The mass balance assumes that the liquid entrained in the foam has the same concentration as the liquid in

the pool and that the enriched solution surrounding the interface is of negligible volume.

$$\Gamma = \frac{Lfd}{6G}(C_F - C_P), \quad (8)$$

where C_F is the concentration in collapsed foam and C_P the concentration remaining in the liquid pool of the contactor, which has equilibrated with the foam. The factor 6/d is the surface area to volume ratio for perfect spheres; rigorously this factor may be closer to 6.3/d to account for the shape of foam bubbles[48].

An alternate method that is more precise at low surfactant concentrations[45] is based on measured depletion of the species of interest in the bulk liquid phase as both bubbles and liquid flow concurrently in a tall column. This technique is not affected by foam coalescence, which in the case of the foaming technique invalidates the assumption that the liquid entrained in the foam has the same concentration as liquid in the pool. In this case, using the symbols of equation 8, the mass balance to derive surface concentration is:

$$\Gamma = \frac{Ld}{6G}(C_{in} - C_E), \quad (9)$$

where C_{in} refers to concentration of the species of interest in the stream entering the contactor, and C_E is the concentration in the bulk liquid that has equilibrated with the rising bubble interfaces. In both equations 8 and 9 the term Γ/d can be calculated independently of the bubble diameters used in the experiment.

In both the foaming method and the liquid-depletion technique, measurements of ion enrichments are most readily carried out using constant flows and inlet surfactant concentrations. Ions of interest are added to solution bringing about changes in ionic strength, affecting equilibria in the following ways:

a) Increased normalities bring about enhancement of of surfactant adsorption due to reduction in electrostatic repulsion at the interface.
b) Constant surfactant concentration in solution with increasing quantities of non-surfactive ions in solution produces changes in the ratio of surfactant counter-ion (non-surfactive ion originally associated with surfactant) to non-surfactive counter-ions of interest.

Interpretation of such experiments should be based on an understanding of these factors. It is also more convenient in several ways to visualize ion enrichment at surfactant-loaded interfaces as an ion-exchange phenomenon than as adsorption.

Capacity for Ion Removal

Figure 4 shows isotherms for cupric-ion sorption at interfaces loaded with an anionic surfactant at different concentrations[38]. The data were measured using the cocurrent-flow technique and a column apparatus and procedure described elsewhere[45]. Constant flows and surfactant concentrations were employed to obtain each isotherm, while changing the cupric ion concentration in solution. The surfactant used was the ammonium salt of an anionic surfactant (Needol 25-3A, Shell Chemical Co.). In this case it was shown in separate measurements that the variation of ionic strength resulting from the experimental procedure did not affect surfactant equilibrium significantly.

The horizontal solid lines labelled A, B, C, in figure 4 denote total capacity for cupric ion uptake. This capacity was calculated independently from the measured number of surfactant equivalents adsorbed during the experiments, converted to a weight-of-copper basis.

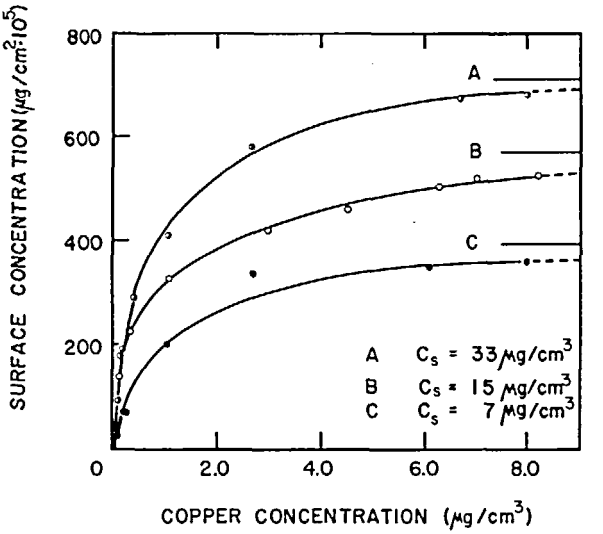

FIGURE 4
Adsorption isotherms for copper (II) at air-liquid interfaces containing Neodol 25-3A. C_s is the surfactant concentration in the bulk liquid, at equilibrium.

Sorption of cupric ions at the surfactant-covered interfaces is nearly complete at a relatively low equilibrium concentration in solution. This indicates specificity for copper uptake over the competing ions present in solution, in this case ammonium and hydrogen.

The direct proportionality between maximum cation-uptake capacity and interfacial concentration of surfactant underscores the advantage of having high interfacial surfactant concentrations to carry out efficient separations. The increasing slopes for increasing surfactant concentrations at low copper content are additional evidence of more favorable copper uptake with increased interfacial concentrations of surfactant.

Comparative experimental data on maximum capacity for cupric ions with different surfactants are given in table 1. For example, taking the highest uptake

TABLE I

MAXIMUM CAPACITY FOR CATION REMOVAL

Reference	Surfactant	Bulk Liquid Surfactant Concentration mM/l	Maximum Surface Capacity $eq/cm^2 \times 10^{10}$
Dick & Talbot (1971) (Batch Cell)	$R\text{-}SO_4Na$ ($R = C_{12}$)	1.8	2.1
Huang & Talbot (1973) (Batch Cell)	$R\text{-}OSO_3Na$ ($R = C_{12}$-)	1.4	2.5
Valdes-Krieg (continuous cocurrent flow)	$R\text{-}(EtO)_3\text{-}SO_3NH_4$ ($R = C_{12}\text{-}C_{15}$)	0.7	2.5

capacity ($\Gamma_{max}=2.5\times10^{-10}$ eq/cm^2) in table 1, one can determine the removals attainable in a single-stage contactor for an idealized case of perfect selectivity for the ion of interest. Solving for removal efficiency (fraction of ion remaining in effluent liquid) using equation 9 gives:

$$\eta = 1 - (C_p/C_{in}) = \frac{6G}{Ld}\frac{\Gamma_{max}}{C_{in}} \qquad (10)$$

Results for removals at different feed concentrations are plotted in figure 5, which shows the factor, $\Lambda=6G/Ld$ as a parameter for the various curves. Applicability of the process using single-stage contact is shown to be limited to low concentrations, determined by the capacity of bubble interfaces for adsorption of surfactant.

In this case the group 6G/Ld is the surface-area to liquid throughput ratio. In actual operation of a

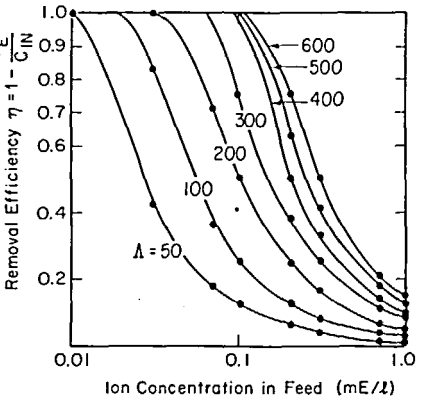

FIGURE 5
Removal efficiencies as a function of counterion concentration in the feed to a single-stage contactor. Sorption capacity, given by surfactant concentration at the interface is 2.5×10^{-10} eq/cm^2. Λ, or extraction factor, is used as parameter for each curve and is defined in the text following equation 10.

contactor one would maximize this ratio to the extent necessary to provide the desired removal capacity. This is done by:

a) Reducing the bubble diameter. Choose a gas sparger with the smallest pores consistent with pressure drops that afford reasonable costs of compressing air. This has also been done by pressurizing solution in the presence of air followed by throttling[16]. It should be noted, however, that smaller bubble diameters give smaller bubble-rise velocities, reducing the gas throughput attainable in a contactor of a given size[13].

b) Increasing the gas flow rate. This is limited by the onset of slug flow in the pool and excessive liquid entrainment in the foam for a given bubble diameter. Liquid entrainment in the foam can be

reduced by allowing sufficient drainage time for the foam before exiting the contactor, either by enlarging the contactor above the pool or by expanding it conically above the pool.

c) Reducing the liquid flow rate. Economical throughputs per unit cross sectional area of contactor are determined by its capital cost. Pilot scale tests in a 1-ft^2 contactor[41] indicate that throughputs of 4-5 gallons per minute per square foot of cross sectional area are possible with good efficiency.

Selectivity

Removal efficiencies of non-surfactive ions pictured in equation 10 and figure 5 reflect the assumption of constant uptake capacity and infinite selectivity for one ion of interest. In any real separation problem solution parameters and competition among ions for uptake at surfactant-loaded interfaces will affect removal efficiencies to various degrees.

Consider the simplest case where the hydrogen form of an anionic surfactant is put into pure water. An example would be hexadecyl sulfonic acid. Solution is fed into a long column and contacted with air bubbles so that a very close approach to equilibrium is attained.

At equilibrium, surfactant ions adsorb on bubble-liquid interfaces, imparting to the bubbles a net surface charge equivalent to an ion-exchange surface. This charge is neutralized by a stoichiometric amount of ions of opposite charge (counterions) that are concentrated in a thin liquid layer surrounding the bubble interfaces. The original solution is now depleted of a significant amount of both surfactant ions and counterion. Having hydrogen ions associated

with the surfactant originally put in solution results in a system with no competing counterion species and thus exhibiting perfect selectivity for hydrogen ion.

Consider now the case where a salt is gradually added to the surfactant solution in the contactor. The following changes occur:

a) There is a gradual increase in surfactant adsorption at bubble interfaces, accompanied by additional depletion of surfactant in the liquid phase. This is the result of increasing solution ionic strength, which reduces electrostatic repulsion between surfactant ions at interfaces.

b) Two counterions are now being attracted to the interface to balance the surface charge created by adsorption of surfactant.

The first effect has rarely been taken into account in foam-fractionation experiments. In some cases (e.g., the results presented in fig. 4) it does not significantly alter surfactant equilibria; significant changes do occur in other systems, however, as will be discussed below. The competition among counterions has been measured for a number of systems, and various theories have been developed to interpret the resulting selectivities.

Empirical Observations: Walling, et al.[47] and Wace and Banfield[13] developed two basic selectivity rules for action uptake based on experimental evidence:

1) Bivalent ions are enriched preferentially over monovalent species. Trivalent ions were not found to be further enriched, an effect ascribed to steric effects of hydrolysis.

2) Among ions of similar valence, enrichment was found to be inversely proportional to ionic radius in solution.

Two approaches can be used to account partially for these observations:

Diffuse Double Layer Theory (DDL): The equations of Chapman and Gouy relate charge and ionic concentration distributions near a charged surface to the attraction of counterions, introducing a Boltzman distribution that has ionic valence as a weighing factor[33]. This model was subsequently extended by Jorné and Rubin[49] to account for the distance of closest approach to the charged interface for different ions. The distance of closest approach used is determined by the hydrated ionic radii of the species in question. The main features of this approach are:

1) The two parameters--valence and hydrated radii--are used to explain separability among counterions.
2) Selectivity is assumed to be proportional to the range of interaction with the charged interfaces. This results in predicting severe decreases in selectivity with increasing ionic strength.
3) From a point of view of correlating data, given parameters such as surface and bulk-liquid concentrations, hydrated radii become adjustable parameters in the model. The values of hydrated radii obtained are dependent on the measurement technique and solution parameters prevailing during measurement[49].

Mass-Action Theory: The similarity between ion sorption at a surfactant-loaded interface and sorption on an ion-exchange resin suggests the use of mass-action relations to correlate ion equilibria. For this purpose the similarity between both processes is drawn upon by assuming the liquid at the interface to be a concentrated solution in contact with a dilute one. The adsorbed

surfactant is assumed to be an immobile part of the solute concentrated at the interface, and counterions are free to migrate from this concentrated solution to the more dilute bulk liquid. Depending on the assumption used to determine the thickness of the concentrated-solution layer surrounding the interface (i.e., thickness of the Stern layer[50] or length of the surfactant ion), the concentration ratio of enriched solution to bulk liquid can be of the order of millions.

Maintaining electroneutrality in the concentrated-solution layer involves balancing the diffusive tendencies and the electrostatic potential exerted on the counterions as they tend to imbalance the immobile charge at the interface. For a multi-ion system a stronger potential is established when an ion of higher valency escapes; therefore, such ions are held more strongly at the interface.

A binary ion-exchange process of this type can be represented as follows[51]:

$$A + \frac{Z_A}{Z_B}(BS_{Z_B}) \underset{}{\overset{K_M}{\rightleftharpoons}} (AS_{Z_A}) + \frac{Z_A}{Z_B} B \qquad (11)$$

where S represents adsorbed surfactant interaction with A or B. A and B are ions of valence Z_A and Z_B in solution, respectively, and AS_{Z_A} and BS_{Z_B} represent the amounts of each counterion sorbed at the interface.

The equilibrium implied in equation 11 can conveniently be expressed as:

$$K_M = \frac{[AS_{Z_A}]}{[A]} \left(\frac{[B]}{[BS_{Z_B}]} \right)^{Z_A/Z_B} \qquad (12)$$

where the symbols now denote surface and bulk concentrations. Use of a subsurface depth, δ, (thickness of enriched liquid surrounding an interface) results in hypothetical volumetric concentrations at the interface, A_S and B_S, given by:

$$[A_S] = \frac{[AS_{Z_A}]}{\delta} \qquad [B_S] = \frac{[BS_{Z_B}]}{\delta}$$

To express bulk liquid concentrations the symbols A_b and B_b are used; so as to give

$$K'_M = K_M \delta^{(Z_A/Z_B - 1)} = \frac{[A_S]}{[A_B]} \frac{[B_B]}{[B_S]}^{(Z_A/Z_B)} \tag{13}$$

The subsurface depth, δ, in this equation is not related to diffuse-double-layer thickness. Diffuse-double-layer thickness is directly affected by ionic strength in the DDL theory, which thereby predicts reduced selectivities at high ionic strengths. For a mass-action expression the effect of ionic strength on equilibria is implied in its formulation. The total amount of counterions sorbed at a surfactant-loaded interface is determined by its uptake capacity, $Z_A[AS_{Z_A}]+Z_B[BS_{Z_B}]$, whereas the concentrations attainable in the bulk liquid can comparatively be considered to be variable.

The following potential advantages can be found in using a mass-action model as compared to the DDL approach:

1) It is simple in its formulation, and therefore allows one to include both bulk-liquid and surface nonidealities into the model and visualize their effect in a simple fashion. Such nonidealities will be discussed further below.
2) It allows a priori qualitative estimates of selectivities for a given system using a particular surfactant. This would be done resorting to equilibrium data in other systems, i.e., solid-liquid ion exchange. Various ways of estimating δ for surfactant equilibria[33,34] can be used for qualitative purposes.

3) The model parameters can be made adjustable to fit simple equilibrium expressions from experimental data. Such an empirical form is a significant improvement over commonly used surface-adsorption isotherms, which neglect the presence of other ions and changing sorption capacities of bubble interfaces.

In using such a relation for correlation purposes one can account for some nonidealities using the following approaches, which are commonly employed in solid-liquid ion exchange[51,52]:

a) Use up to three adjustable parameters (K_M, Z_A/Z_B, δ).

b) Approximate the system by a constant separation factor ($Z_A/Z_B=1$) for a limited range of concentrations. This alternative would be used when a complex operation is modeled (e.g., back-mixing in a tall column or multistage modeling).

Limitations: Practical application of the above models results in incomplete agreement with experimetal data. This might be expected from the various nonidealities encountered in electrolyte solutions, particularly in the enriched portions near air-liquid interfaces.

Figure 6 shows selectivity for copper ions in the presence of ammonium, sodium and hydrogen ions, as measured in the cocurrent-flow system where the surfactants are salts of these ions and a surfactant anion (Neodol 25-3A). The data are presented as a log-log plot of distribution coefficients for each ion in each binary system. This representation enables one to determine Z_A/Z_B as the slope of the experimental data and K_M as the intercept, using the mass-action model (equation 13). The three curves show a limitation of the mass action model in that the indicated ratios of

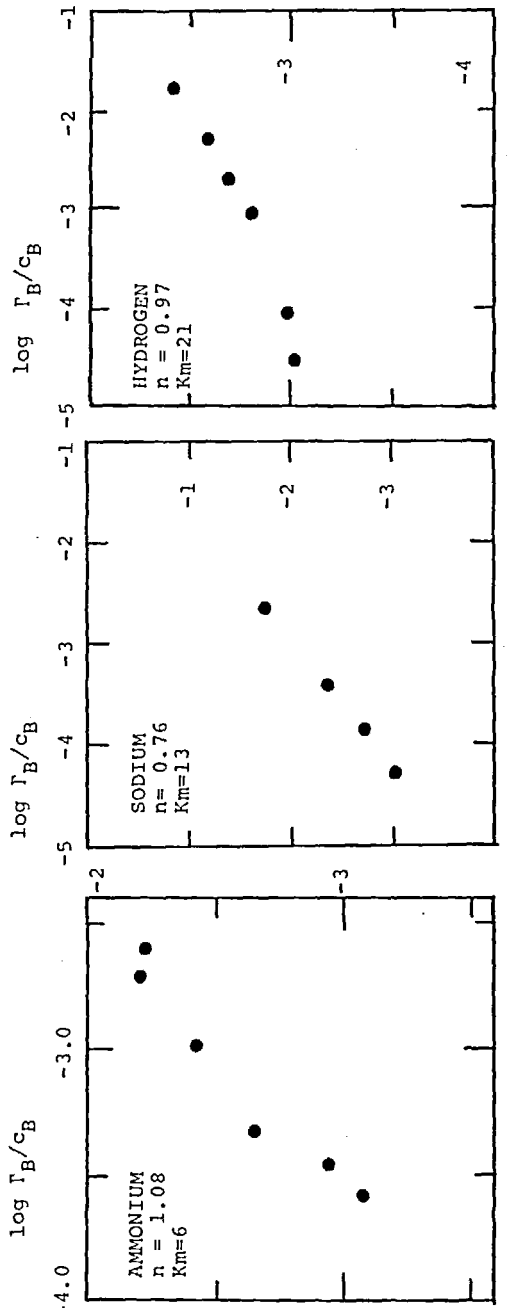

FIGURE 6. Empirical determination of mass action constant K_M and valence ratio Z_A/Z_B from experimental data (see equation 12). Species B for each plot is the monovalent ion originally associated with the surfactant, as indicated in each diagram. Γ represents surface concentration (moles/cm^2), c represents concentration in the bulk (moles/cm^3).

valencies determined from the slopes for the three systems are significantly less than 2.0, which would correspond to monovalent/divalent systems. Such behavior has often been observed in solid-liquid ion exchange. Using the empirically determined valence ratios (Z_A/Z_B), the mass-action constants determined do conform with observed selectivities for cupric ions, which increase in the order $NH_4^+ < Na^+ < H^+$.

Specific Interactions

1) Ion Pair Formation: Figure 7 shows typical experimental data for the copper-hydrogen binary equilibrium with Neodol 25-3H (ion-exchanged to the hydrogen form) determined by the authors[38]. Salient features of these data, measured through the cocurrent liquid-depletion technique described above, are:
   a) Using constant surfactant concentration and operating conditions, the addition of cupric salt (sulfate) results in a large initial enhancement of surfactant adsorption. Surfactant adsorption then remains relatively constant as the copper concentration at the interface comes closer to stoichiometric equivalence with the surfactant at the interface.
   b) The surface tension of the solution becomes lower with increasing copper normality. This behavior parallels the increasing surface concentrations shown in figure 7, i.e., a large initial lowering of surface tension followed by small decreases at higher copper concentrations.

   Further experiments using smaller cupric ion additions to expand the initial concentration region supported the conclusion that surfactant-adsorption enhancement is caused by copper adsorption rather than by increased ionic strength of the bulk liquid.

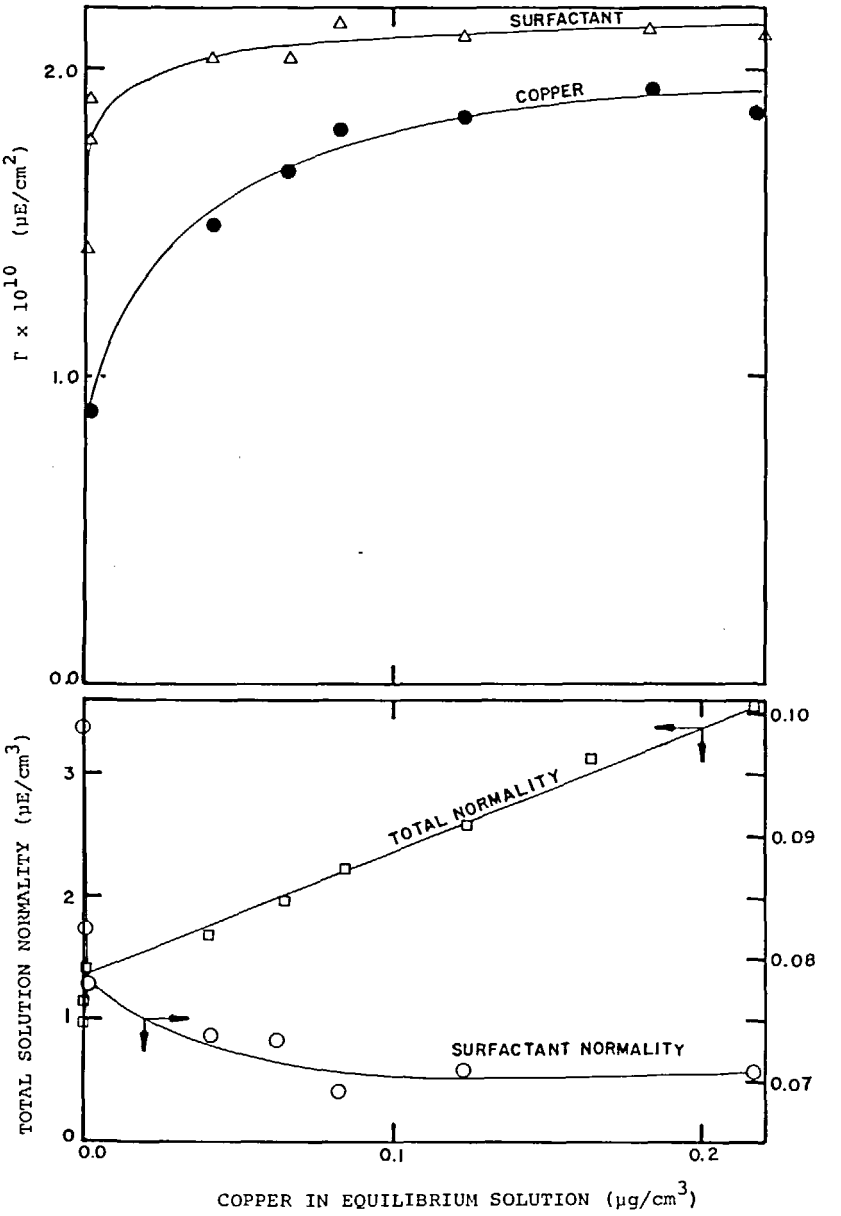

FIGURE 7
Adsorption of cupric ion using hydrogen-Neodol: solution and interfacial concentrations.

Figure 8 shows copper-hydrogen equilibrium data determined by the same procedure using constant surfactant and copper concentrations but adding hydrogen ion in the form of sulfuric acid to strip the copper ion from the bubble interfaces[38]. Copper sorption at bubble interfaces is not affected by a large excess of monovalent ion to the extent predicted by electroselectivity alone. Sorption of cupric ions was not significantly affected by hydrogen ion up to about 20:1 excess over copper ions. For concentrations of hydrogen ion above this level there is gradual replacement of copper ions at the interface by hydrogen ions. Notice that hydrogen-ion concentration is given in the figure with logarithmic coordinates; therefore the actual separation factor for copper ions (ratio of equivalent fraction at the interface to equivalent fraction in the bulk liquid for copper, divided by the same ratio for hydrogen) is increasing, although surfactant utilization for copper removal is lower.

Similar experiments were conducted for copper using the sodium form of Neodol and adding sodium ion in large excess over copper ion[38]. A behavior similar to the copper-hydrogen system was observed, although a smaller excess of sodium ions resulted in replacement of copper ions at the interface by competing sodium ions. These results indicate a lesser effect of monovalent ion excess than that observed by Dick and Talbot[53]. The difference in the case of sodium ions could be ascribed to sensitivity of measurement technique and/or the surfactant used in Dick and Talbot's work, which was sodium lauryl sulfate.

The results described above indicate feasibility of recovering certain divalent ions from solution,

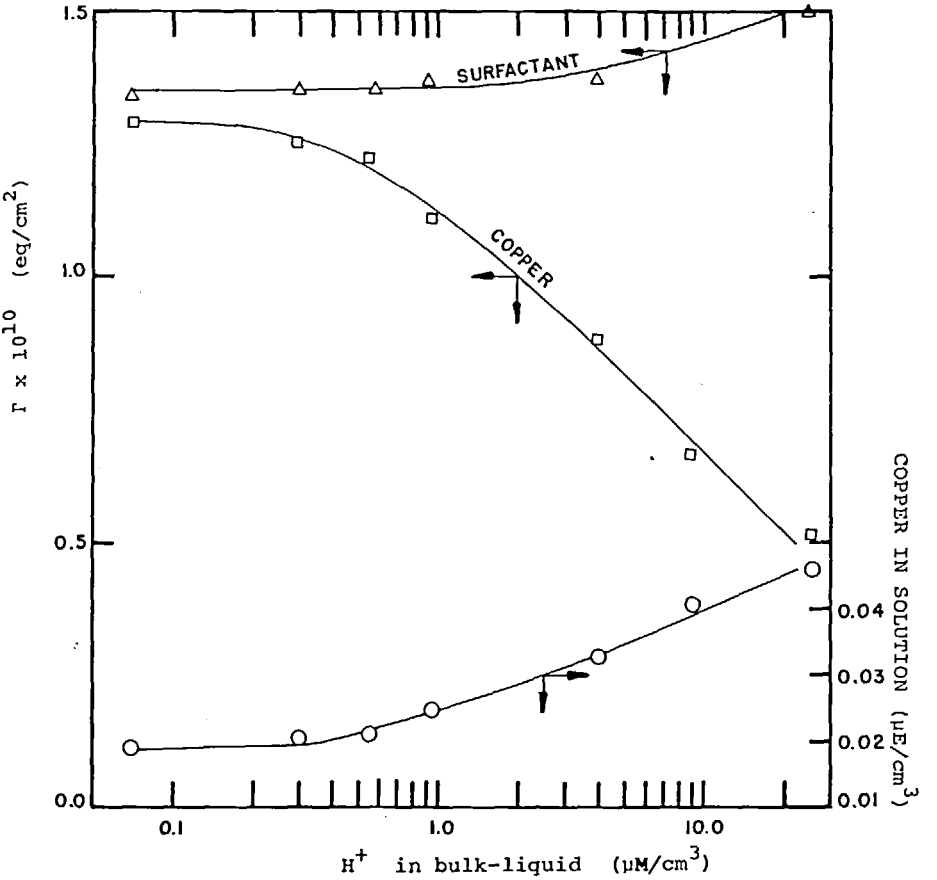

FIGURE 8
Effect of pH on copper (II) uptake.

even if they are present in conjunction with a large excess of monovalent ions. The authors[38] were able to recover a significant portion of copper present at 1 ppm in 1.9 N sodium chloride brine and to a lesser extent from three-fold concentrated seawater, using combined foam and bubble fractionation as described below.

From an equilibrium point of view, one can interpret the above findings as a specific interaction between surfactant and cupric ions not accounted for by electroselectivity. In order to represent it quantitatively, one could postulate for simplicity the formation of an ion pair at the interface in conjunction with electroselectivity as explained through a mass-action relationship.

2) Surfactant Dissociation: Experimental evidence obtained by the present authors[38] indicates that, for solutions of surfactant salts of different monovalent electrolytes, the surface enrichment of surfactant at constant bulk surfactant concentration differed according to the monovalent ion originally associated with the surfactant anion. Thus, for the sodium, ammonium and hydrogen forms of Neodol 25 adsorption increased in the order hydrogen<sodium<ammonium, which would correspond inversely with hydrated radius of the cation in solution. A behavior like this was also observed by Matuura and coworkers[42] and could be indicative of stronger surfactant interaction at the interface with given cations, resulting in diminished electrostatic repulsion at the interface and enhanced adsorption.

3) Hydrolysis at Interface: Certain cations undergo hydration steps as the solution environment becomes more basic. Bulk and interfacial compositions can be sufficiently different to lead to hydrolysis of a cation at the interface even if the bulk liquid is quite acidic. Such phenomena have been recognized by Huang and Talbot[54] in their work with lead, calcium and cadmium ions, by Rubin, et al.[55] and by Jacobelli-Turi, et al.[22]. The present authors[38]

observed indications of hydrolysis effects with divalent cobalt and nickel ions using the hydrogen form of Neodol. Partial hydrolysis of divalent ions results in reduction of the effective valence for competition against other ions for sorption at the interface. This effect manifested itself differently for cobalt and nickel ions, as shown in fig. 9:

a) Cobalt ion sorption at interfaces increased with increasing cobalt ion in solution to the point of exceeding the stoichiometric capacity of the

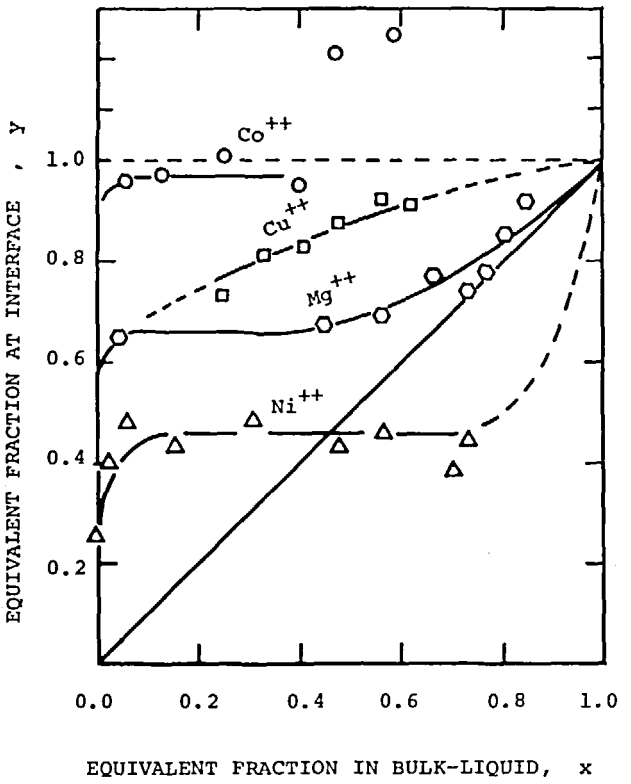

FIGURE 9
Experimental equilibrium behavior: binary systems.

surfactant-loaded interface. This suggests that the first hydrolysis product of cobalt ions still competes favorably with hydrogen ions for sorption at surfactant-loaded interfaces.

b) Nickel ions, which have a larger hydrolysis constant than cobalt ions, exhibited a different sorption behavior than that for cobalt. After sorption with high selectivity for low nickel ion concentrations, the sorption levelled off at a level of about half the sorption capacity of the surfactant-loaded interfaces. This suggests unfavorable competition for the monovalent nickel ion hydrolyzate against hydrogen ion in solution.

The non-idealities described above were included in a model that accounted for them in conjunction with electroselectivity to analyze concurrent flow experiments[38]. Results of this model using order-of-magnitude estimates for the various constants involved (mass action and dissociation) resulted in shapes of distribution diagrams (equivalent fraction in bulk liquid against equivalent fraction at interface) that approximated the experimental results shown in fig. 9. Independent estimates of such parameters could conceivably permit a reasonable a priori prediction of binary and multicomponent equilibria. Correlation of cation equilibria in this way would be a first step towards obtaining equilibrium expressions useful in process-screening design.

CONTACTOR DESIGN AND ANALYSIS

Foam vs. Bubble Fractionation

Early work on foaming processes for the removal of metal ions from aqueous solutions dealt primarily with the goal of removing traces of radioactive substances (see, for example, Schnepf, et al.[31], Haas and Johnson[9],

and Arod[56]. In all cases, the contactor used was a tall column filled with foam. Several investigators (e.g., Haas and Johnson[9]; Jashani and Lemlich[57]) have used plug-flow mass-transfer equations to estimate rates of equilibration between downflowing liquid drainage and rising foam in countercurrent contactors. The results indicate high rates of mass transfer for surfactant transport to the foam-bubble interface. For reasonably high foam columns, the removal is closely approximated by postulating equilibrium between the rising foam and the downflowing liquid at all points in the column and plug flow for both phases.

There are two important disadvantages of foam columns when applied to removal of surfactants or other dilute solutes from relatively large water streams. One is that the liquid throughput is limited by the drainage rates of foam, which are quite small. This calls for contactors of large cross-section areas, with attendant problems of achieving flow uniformity across the cross-section. The other problem relates to maintaining foam stability. The surfactant concentration at the air-entry point (bottom of the column) must be high enough to generate a foam. This limits the degree of removal of surfactant that can be attained. Furthermore, surfactant concentrations required for foam stability are often close to the critical micelle concentration, which can lead to the presence of surfactant and micelles (surfactant agglomerates) in solution. Micelles are probably not adsorbed on bubbles. They therefore represent surfactant that is not effective for pairing at the bubble interface with the solutes to be removed, and an additional contamination in effluent streams.

These problems can be overcome by the use of combined bubble and foam fractionation, depicted in fig. 10. The

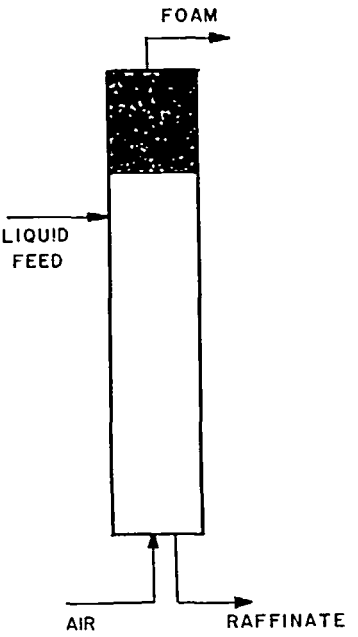

FIGURE 10
Combined bubble and foam fractionation.

column is largely filled with aerated liquid, through which fine bubbles rise after being released at the bottom. The feed is introduced into this aerated liquid section, and a foam forms on top of the bubble section, above the feed point. The products are the collapsed foamate and a raffinate withdrawn from the bubble section. Enrichment of surface-active and co-adsorbed species will occur in the foamate, giving depletion of the raffinate product. Furthermore, if the length/diameter ratio of the bubble column is sufficiently large, with the liquid feed entering the top of the bubble section and the raffinate withdrawn from the bottom of the column, additional separation can occur by countercurrent stripping in the bubble section. An

example of the additional separation attainable in this way for surfactant removal is shown in fig. 16 (below), where it can be seen that a considerable axial concentration gradient developed within the liquid phase. An anionic surfactant (Neodol 25-3A) in concentrated brine was used in this case.

Modeling of the Separation Attained

A proper analysis of the separation attained in combined bubble and foam fractionation must allow for the net rates of upflow and downflow of liquid, equilibrium surface enrichments for given ranges of bulk-liquid concentrations, rates of solute mass transfer from the bulk liquid to the bubble interfaces, and axial dispersion within the bulk liquid and surface phases. Extension of the analysis to account for foam coalescence is straightforward but was found to be of little practical significance for surfactants showing favorable equilibrium and/or at low concentrations. The appropriate differential equations and boundary conditions describing this situation will now be developed:

It is convenient to express surface concentrations, Γ (moles per unit interfacial area), in terms of an equivalent gas-phase concentration, C_y (moles per unit gas volume), as follows:

$$C_y G = \Gamma A \tag{14}$$

The surface area throughput rate, A, divided by the volumetric gas flow rate, G, is 6/d, where d is the Sauter mean bubble diameter. Hence we have

$$C_y = 6\Gamma/d \tag{15}$$

As is shown in fig. 11, the volumetric liquid feed flow, L, is ultimately split into a foamate fraction, T, and a bottoms raffinate stream, Q. Considering net flows of gas and liquid, the section above the liquid feed is cocurrent, and the section below the feed is

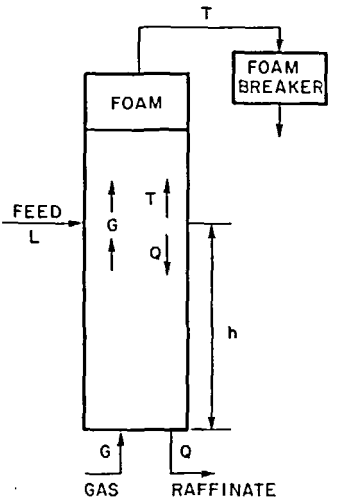

FIGURE 11
Flows in combined bubble and foam fractionation.

countercurrent. For the section below the feed, a mass balance allowing for axial dispersion gives

$$-SE_x \frac{d^2C_x}{dz^2} + Q \frac{dC_x}{dz} = G \frac{dC_y}{dz} + SE_y \frac{d^2C_y}{dz^2} \qquad (16)$$

where S is the column cross-section area, C_x is liquid concentration, z is axial distance along the column, and E_x and E_y are liquid- and gas-phase axial dispersion coefficients, respectively. z is taken to be positive downwards. Local flows in excess of the net flow rates are taken up in the axial dispersion coefficients.

A similar balance for the aerated liquid section above the feed gives

$$SE_x \frac{d^2C_x}{dz^2} + T \frac{dc_x}{dz} = -G \frac{dC_y}{dz} - SE_y \frac{d^2C_y}{dz^2} \qquad (17)$$

It will be assumed that the foam height above the aerated liquid is low enough not to give any further enrichment in the foam section of the column.

If finite rates of mass transfer of the solute between the liquid bulk and the interface are to be allowed for, additional equations are required, relating to the two sides of equations 16 and 17 to products of mass-transfer coefficients, interfacial areas per unit volume, and concentration-difference driving forces. These equations are given elsewhere[38], in a form that also allows for two liquid feeds at different levels in the bubble zone. An analytic solution was found for the case of a linear equilibrium relationship between C_y and C_x. A computer solution was developed for the case of a more general equilibrium relationship. Valdes-Krieg[38] reports specific solutions for various combinations of the independent variables in the case of an equilibrium relationship expressable through the Langmuir adsorption isotherm.

Experimental measurements in various bubble fractionation systems[38,45] and correlations of mass transfer to bubbles in the absence of interfacial resistance indicate that the assumption of infinitely fast mass transfer is satisfactory for column analysis in many situations. This assumption corresponds to postulation of local equilibrium between interface and bulk liquid, and is most satisfactory for cases of small bubbles (e.g., 1 mm or less) and relatively high liquid pools (e.g., 120 cm or more). Under this assumption, C_y and C_x are related through the experimental equilibrium relationship:

$$C_y = g(C_x) \tag{18}$$

Also, with the assumption of infinitely rapid mass transfer, equation 17 drops out, since there can be no

further equilibration in the cocurrent section. C_x and C_y are therefore constant in the liquid section above the feed.

Two boundary conditions are required for the solution of equations 16 and 18. One of these is a mass balance at the bottom of the column ($z=h$). Liquid leaving the column must have the same composition as that inside the column at the bottom, and the bubble interfaces must load immediately upon entry to equilibrium with the bulk liquid, because of the assumed infinitely rapid mass transfer. Hence the quantity of mass transfer to the bubbles must be offset by solute input by axial dispersion:

At $z=h$,

$$SE_x \frac{dC_x}{dz} + SE_y \frac{dC_y}{dz} + GC_y = 0 \qquad (19)$$

At the feed point ($z=0$), there is no axial dispersion upward because of constant concentrations in both phases above the feed. Also, the bulk liquid concentration and the corresponding bubble interface concentration should not undergo discontinuities in absolute value. Hence the solute input in the feed can be equated to the combined effects of convection with the net flows upward and downward (T and Q) and of axial dispersion downward:

At $z=0$,

$$SE_x \left.\frac{dC_x}{dz}\right|_{z=0^+} + SE_y \left.\frac{dC_y}{dz}\right|_{z=0^+} - QC_x - TC_x + LC_{in} = 0 \qquad (20)$$

or

$$SE_x \left.\frac{dC_x}{dz}\right|_{z=0^+} + SE_y \left.\frac{dC_y}{dz}\right|_{z=0^+} + L(C_{in} - C_x) = 0 \qquad (20a)$$

Linear Equilibrium: An analytic solution to equation 16 is obtained with equations 19 and 20 as boundary conditions if equation 5 is replaced by a linear equilibrium relationship:

$$C_y = \frac{6\Gamma}{d} = mC_x \tag{21}$$

The solution is

$$\frac{C_x}{C_{in}} = \frac{1 - \Lambda\exp[\lambda(1 - z)]}{1 - \Lambda[(1 - f)(\Lambda - 1) + 1]\exp\lambda} \tag{22}$$

where

$$\lambda = Pe_{ox}(\Lambda - 1) \tag{23}$$

$$\Lambda = \frac{mG}{Q} \tag{24}$$

$$f = \frac{T}{L} = \text{foamate fraction} \tag{25}$$

$$Z = \frac{z}{h} \tag{26}$$

$$Pe_{ox} = \left(\frac{1}{Pe_x} + \frac{\Lambda}{Pe_y}\right)^{-1} \tag{27}$$

$$Pe_x = \frac{Qh}{SE_x} \tag{28}$$

$$Pe_y = \frac{Gh}{SE_y} \tag{29}$$

The raffinate and foamate concentrations, C_R and C_F respectively, are thereby given by

$$C_R = C_{in}\left[\frac{1 - \Lambda}{1 - \Lambda[(1 - f)(\Lambda - 1) + 1]\exp(\lambda)}\right] \tag{30}$$

and

$$C_F = C_{in}\left[\frac{1 - \Lambda\exp(\Lambda)}{1 - \Lambda[(1 - f)(\Lambda - 1) + 1]\exp(\lambda)}\right]\left(1 + \frac{1-f}{f}\Lambda\right) \tag{31}$$

In the extreme of f→0, this analysis is completely analogous to the situation of a single-section extraction process with axial dispersion in both phases but with infinitely rapid mass transfer. As expected, equation 22 for f=0 reduces to the solution for that situation that is given as Case 9 by Miyauchi and Vermeulen[58].

Analyses for bubble fractionation with infinitely rapid mass transfer and linear equilibrium have also been presented by Bruin, et al.[30], Cannon and Lemlich[59]

and Kwon and Wang[60]. However, their solutions postulate as a boundary condition that the liquid concentration at the feed level of the column is the same as that of the feed itself. This assumption is incorrect in view of the dilution of feed accomplished by axial mixing of the feed with less concentrated solution from below. Note also that equation 22 does not reduce to $C_x=C_{in}$ for z=0. As is also the case for liquid extractors and other separation devices showing substantial axial mixing, experimental axial concentration profiles for bubble fractionation columns show an appreciable concentration "jump" ($C_x<C_{in}$) at the feed level; see, for example, the profiles shown in figures 16, 17 and 20, below.

For the limit of infinitely rapid mass transfer an overall Peclet number, Pe_{ox}, is obtained and involves the Peclet numbers for each phase (Pe_x and Pe_y) added reciprocally and weighted by the extraction factor, Λ (additivity of resistances). Consequently, gas-phase axial dispersion dominates at high values of the extraction factor, while liquid-phase axial disperson dominates at low values of the extraction factor. Also, for a separation that is controlled by axial dispersion in the bulk liquid, increasing extraction factors will make the separation attained less sensitive to the degree of axial dispersion in the column. These results are illustrated in figures 12 and 13, which show the separation predicted by equations 30 and 31 as a function of Λ and Pe_x for cases of $Pe_y \to \infty$ and $Pe_y=Pe_x$, respectively. For axial dispersion in the raffinate phase only (figure 12) the separation at high extraction factors is insensitive to axial mixing down to relatively low values of Pe_x. For the case of equal Peclet numbers (fig. 13) efficient countercurrent separation takes place only at quite high values of the

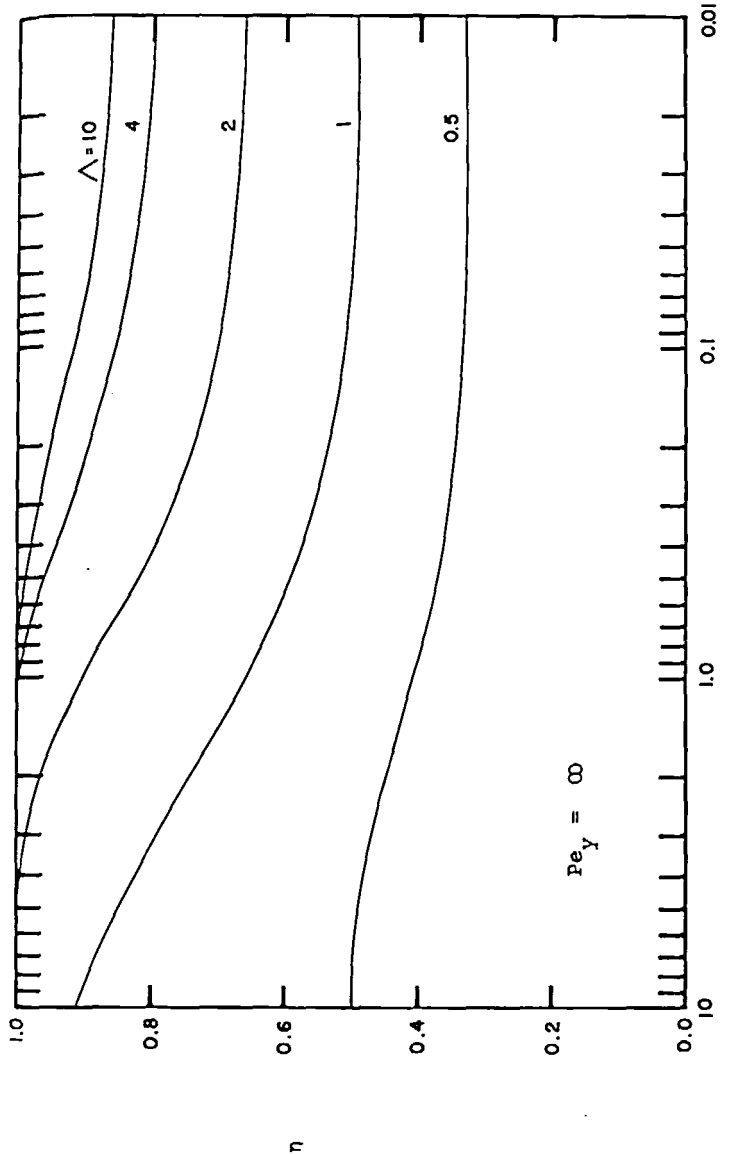

FIGURE 12
Fraction of solute removed (η) as a function of Λ and Pe_x for linear equilibrium, infinitely rapid mass transfer and Pe_y=0.

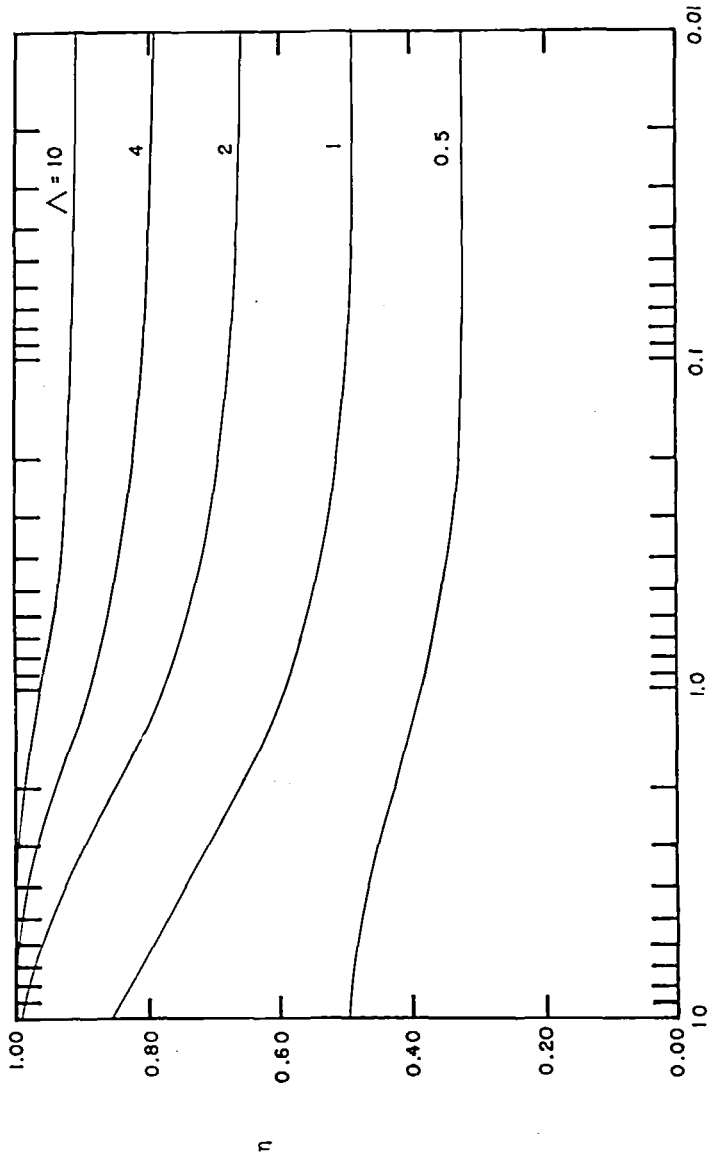

FIGURE 13
Fraction of solute removed (η) as a function of Λ and Pe_x for linear equilibrium, infinitely rapid mass transfer and $Pe_y = Pe_x$.

peclet numbers. The asymptotic separation approached at very low Peclet numbers in both cases corresponds to single-stage equilibration, which is the limit of extreme axial mixing or low column length/diameter ratio.

General Equilibrium Expression: A more general graphical or numerical solution can be developed for the case where C_y is some non-linear function of C_x. Such a situation occurs for most removal processes of interest, since the surface tends to saturate and dC_y/dC_x becomes much less at higher values of C_x. The linear approximation is appropriate usually only for values of C_y far below saturation, or for very low values of C_x.

The method is analogous to the procedure developed by Rod[61] for the graphical solution of the performance of countercurrent solvent extractors, affected by axial dispersion. It will first be derived for the case of zero foamate fraction (f=0) and for negligible axial dispersion in the gas or interface species (E_y=0). It will then be extended to the more general case.

It is convenient to define a new variable, X, which may be considered as a pseudo-liquid composition and which is given by

$$X = C_x - \frac{SE_x}{Q}\frac{dC_x}{dz}$$

$$= C_x - \frac{1}{Pe_x}\frac{dC_x}{dz} \qquad (32)$$

Substitution of this definition of X into equation 16 with E_y=0 yields

$$Q\frac{dX}{dz} = G\frac{dC_y}{dz} \qquad (33)$$

which indicates a straight-line relationship between C_y and X. Substitution of equation 19 as a boundary condition gives the equation for this straight line as

$$C_y = \frac{Q}{G}(X - C_R) \qquad (34)$$

since $C_{y,in}$=0.

Equation 34 extended to the feed level (z=0) also satisfies the other boundary condition, equation 20a. With Q=L (f=0), $X=C_{in}$ at z=0.

Turning now to fig. 14, a graphical construction can be made in the form similar to a common operating diagram. C_y is plotted as the vertical axis, and the horizontal axis represents both C_x and X. The equilibrium relationship between C_y and C_x (equation 18) is shown as the curve stemming from the origin. Equation 34 serves as a pseudo-operating line, located to the right of the equilibrium curve. By virtue of the postulate of infinitely rapid mass transfer, the true operating curve is coincident with the equilibrium curve; however the construction will be made using the pseudo-operating line, as follows:

If G, Q, the equilibrium relationships, E_x, S, C_{in} and h are specified, the calculation starts with an assumed value of C_R, thereby overspecifying the column. The pseudo-operating line is now drawn using equation 34. The composition, at the feed level are given by the specified value of C_{in} (equals X at z=0), and the C_y coordinate of the pseudo-operating line at $X=C_{in}$. C_x at z=0 is then given by the C_x coordinate of the equilibrium curve at this value of C_y.

The column height is divided into n sections of equal height. The change of C_x across any one section is obtained from equation 32, approximated by a finite difference expression for the derivative:

$$\Delta C_x = - Pe_x \, \Delta Z (X - C_x) \qquad (35)$$

where $\Delta Z=\Delta z/h=1/n$. Therefore a staircase construction can be made, where the horizontal distance $(X-C_x)$ is measured and a proportional horizontal distance, ΔC_x, equal to $(Pe_x/n)(X-C_x)$, is measured off to the left of the equilibrium curve. The left-hand end of this line

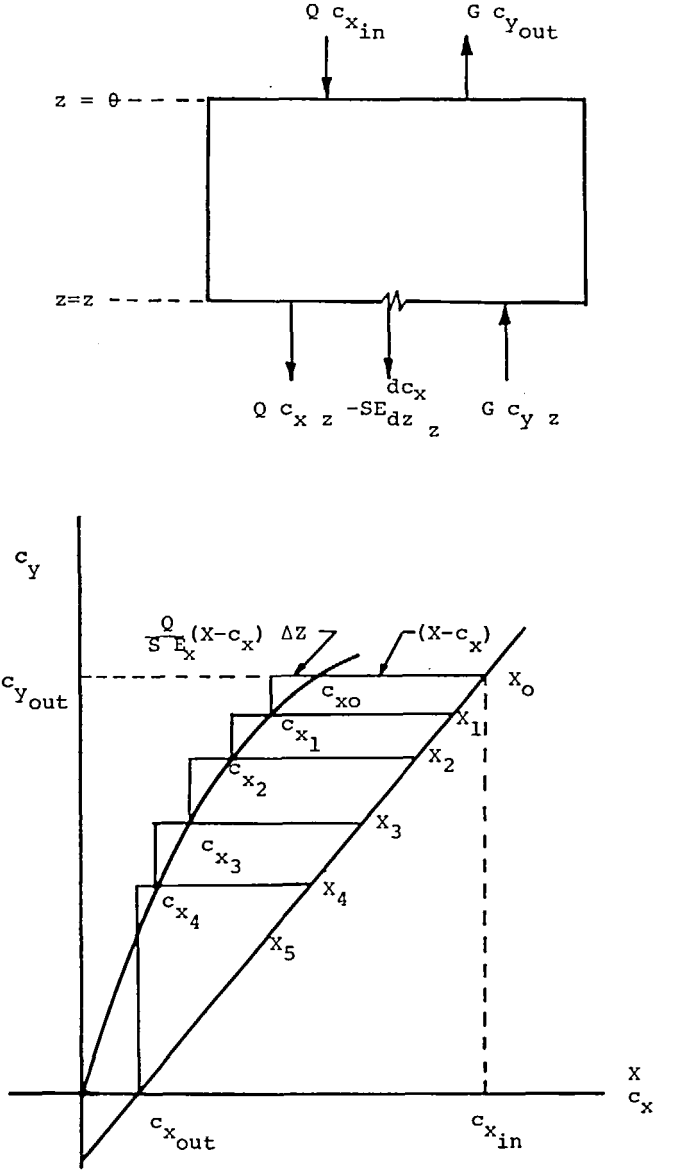

FIGURE 14
Graphical construction for separation obtained during bubble fractionation with infinitely rapid mass transfer, $Pe_y=0$, and f=0.

gives the value of C_x at the end of the increment, and a vertical back down to the equilibrium curve gives the value of C_y at the end of the increment. The construction is then repeated n times.

If, after n steps, the calculated value of C_R equals the assumed value, the solution is complete. Otherwise a higher or lower value of C_R, depending upon the direction of mis-match, is assumed and the construction is repeated. Iteration continues in this fashion until convergence is obtained. The step size can also be decreased (n increased) to ensure a sufficiently close numerical approximation in equation 35.

It should be pointed out that, in general, substituting a specification of C_R for the specification of h does not eliminate the need for iteration, because in that case Pe_x is not known beforehand.

From an examination of fig. 14, it can be seen that the construction has the feature of other, more familiar, operating diagrams in that the change in C_x per increment of height is smaller when the pseudo-operating line is closer to the equilibrium curve. Furthermore, tangency of the pseudo-operating line and the equilibrium curve corresponds to an infinite column height, and crossing of the two curves corresponds to a separation that cannot be achieved with the specified flows.

The calculation has been illustrated for f=0 and E_y=0. The first of these restrictions is easily removed by creating a second mass-balance expression given by equation 34 with L replacing Q, and written for the feed level, z=0;

$$(C_y)_{z=0} = \frac{L}{G}(C_{in} - C_R) \qquad (36)$$

Equation 36 is used to locate the $(C_y)_{z=0}$, C_{in}(=X at z=0) point to start the construction after the assumption of C_R. Equation 35 is then used, unchanged and

in the same fashion as before, for the construction of all the remaining steps.

Removal of the restriction that $E_y=0$ is more difficult. One approach is to carry out the construction for $E_y=0$, and then to obtain an approximation for the E_y term in equation 16 for each increment using the actual value of E_y and the indicated functionality between C_y and z from the $E_y=0$ construction. The procedure can then be repeated iteratively. Another way to carry it out is to use an overall Peclet number based on the slope of the equilibrium line at the point of interest (equation 27). As was noted for the linear-equilibrium solution, the assumption of $E_y=0$ is better for low values of the extraction factor.

The finite-difference graphical procedure can be converted in straightforward fashion to a numerical, computerized calculation. In that case it is also possible to use a higher-order approximation to equation 32 than that given by equation 35.

Figure 15 shows axial concentration profiles, operating lines, and overall separations calculated using the graphical procedure for the case of a typical surfactant equilibrium relationship and for constant flows, axial liquid-phase dispersion, and column height with different feed concentrations (C_{in}). The feed concentrations are denoted by arrows on the right-hand axis. The results show the considerable effect of isotherm curvature on the separation obtained. Some general conclusions from the analysis shown in fig. 15 are the following:

a) For a given isotherm, increasing feed concentration results in less percent change in liquid concentration, both overall and axially along the column height. At very high feed concentration

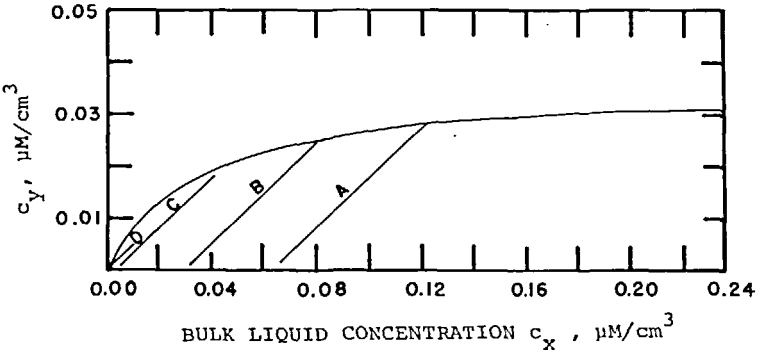

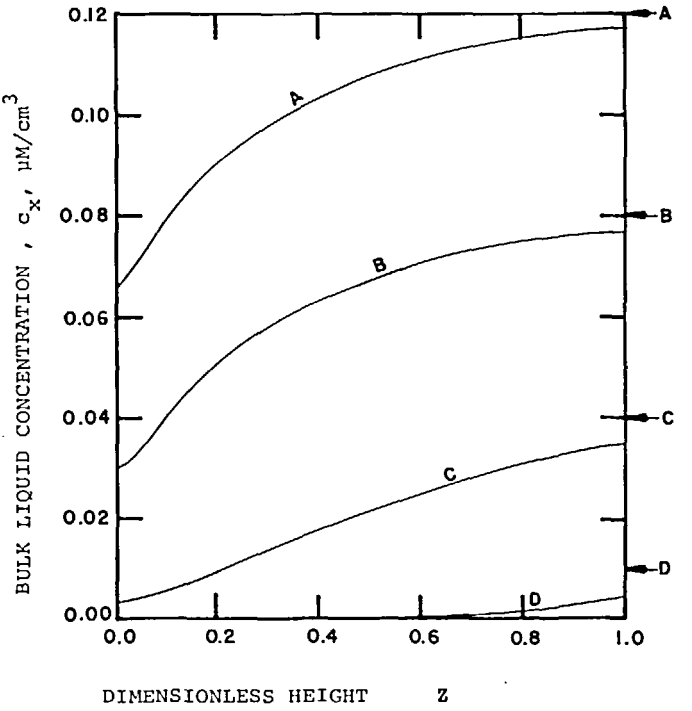

FIGURE 15
Operating diagrams and calculated removals and axial concentration profiles for bubble fractionation with non-linear equilibrium and different concentrations of copper in the feed.

the separation and concentration profile give the appearance of operation with a very large amount of axial dispersion. This phenomenon may be responsible for frequent conclusions in past work that the liquid pool of a foam fractionator functions as if it were well mixed, even for rather large ratios of length to diameter.

b) As for the case of linear equilibrium, C_x at the feed level is lower than C_{in} because of axial dispersion. For the curved isotherm the percentwise difference between these two concentrations increases as the feed concentration decreases, giving an artificial appearance of more axial dispersion at lower feed concentrations.

Improved Design for Counterion Removal

Removal of copper present at 0.5 to 1.0 ppm in high-salinity solutions is of interest because of the presence of copper corrosion product in the effluent brine from evaporation sea-water desalination plants[62]. Experimental tests of copper removal from high salinity solutions have been made using a 6.95-cm inside-diameter bubble and foam fractionation column described elsewhere[45,63,64].

Figure 16 shows the concentration profile observed for the ionic surfactant Neodol 25-3A (see above), for a 5-ft. column height below the feed level, for a liquid superficial velocity of 0.33 cm/sec and G/L of 1.88, volumetric basis, with the feed containing 19.6 ppm Neodol and 1.9 N sodium chloride. Over 98% removal of Neodol is obtained. The concentration profile, obtained from axial liquid samples, can readily be fit through the analysis of column operation presented above. Notice that there is a substantial difference between C_x at the feed level (10.4 ppm) and C_{in} (19.6 ppm).

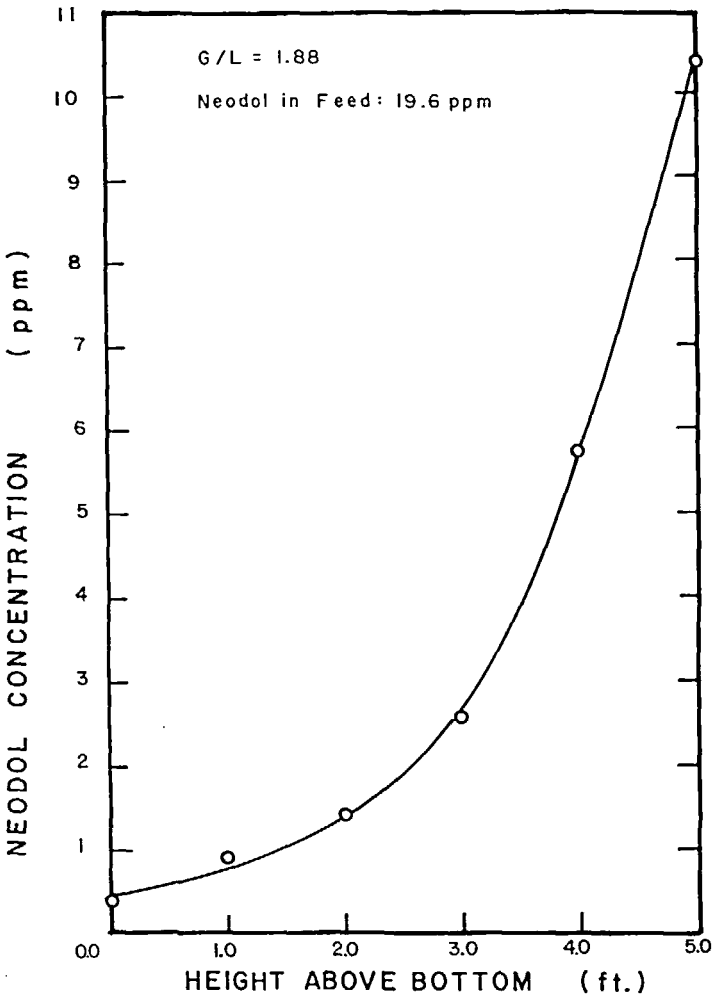

FIGURE 16
Axial concentration profile determined experimentally for combined bubble and foam fractionation in 6.95-cm diameter column, with surfactant added to the main feed.

Figure 17 shows the removal and axial concentration profile obtained for 0.76 ppm copper in the feed (as sulfate) under the same conditions of flow and Neodol

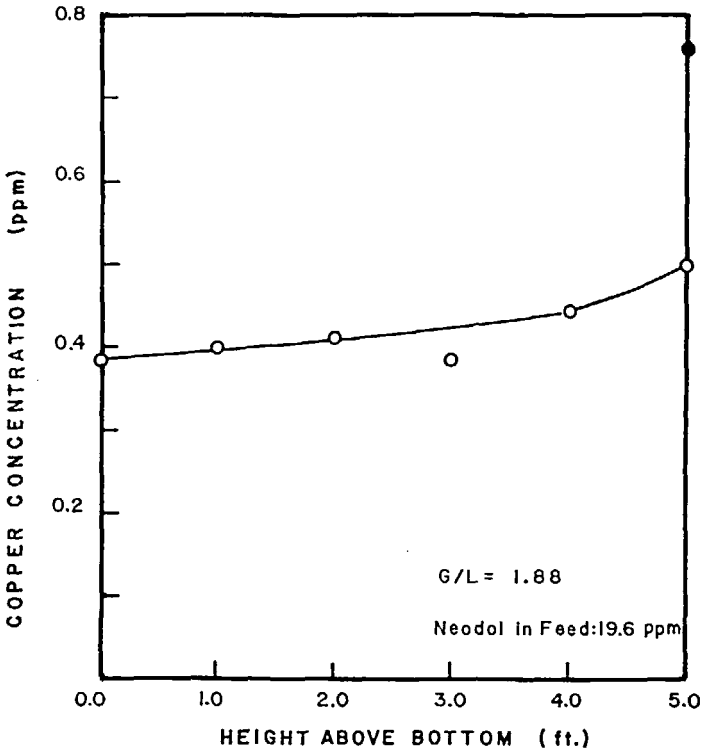

FIGURE 17
Axial concentration profile determined experimentally for copper under the same conditions used in figure 16.

concentration. The copper removal is of the order of 50%, being mostly obtained upon entry of the feed with little added depletion of copper lower in the column. There is an interaction between the axial profiles for Neodol and for copper; the great reduction in Neodol concentration lower in the column considerably reduces the surface capacity for copper at the lower levels. It is interesting to observe that the 50% removal of dilute copper still reflects the extremely high selectivity for adsorption of copper ion over the much more concentrated sodium ion.

A more effective approach for ion recovery from a feed stream[63] is to add a concentrated stream of surfactant at a point in the column considerably below the level of the main, ion-bearing feed. The surfactant must rise from its feed point to the top of the column and thus will appear in substantial concentration at all levels above the lower feed level of concentrated surfactant. This provides greater surface capacity for copper removal in the region above the surfactant feed and below the main, ion-bearing feed. The residual surfactant can be removed from the raffinate by incorporating an additional column section below the surfactant feed, or by using a second, subsequent column.

Figure 18 (right-hand side) shows typical removals and axial concentration profiles predicted for copper in the presence of Neodol, using the graphical method for two cases. In Case 1 the surfactant concentration is constant along the column, such as might be obtained with the separate lower feed of surfactant. In Case 2 the same amount of surfactant is fed (5.6 ppm in the total liquid feed) and the flows are the same, but the surfactant is supplied entirely with the main feed, and the surface capacity at each level is derived from the calculated profile for the surfactant, using the same graphical approach. The left-hand side of fig. 18 shows the construction for this latter case, with each step being made to a lower isotherm as the position within the column becomes lower. Notice that Case 1 gives substantially greater removal than Case 2, and that the axial copper concentration profile predicted for Case 2 is very similar in form to that observed in fig. 17.

Figure 19 shows the graphical construction and the resultant profiles predicted for cases where the surfactant concentration is taken to be constant axially and

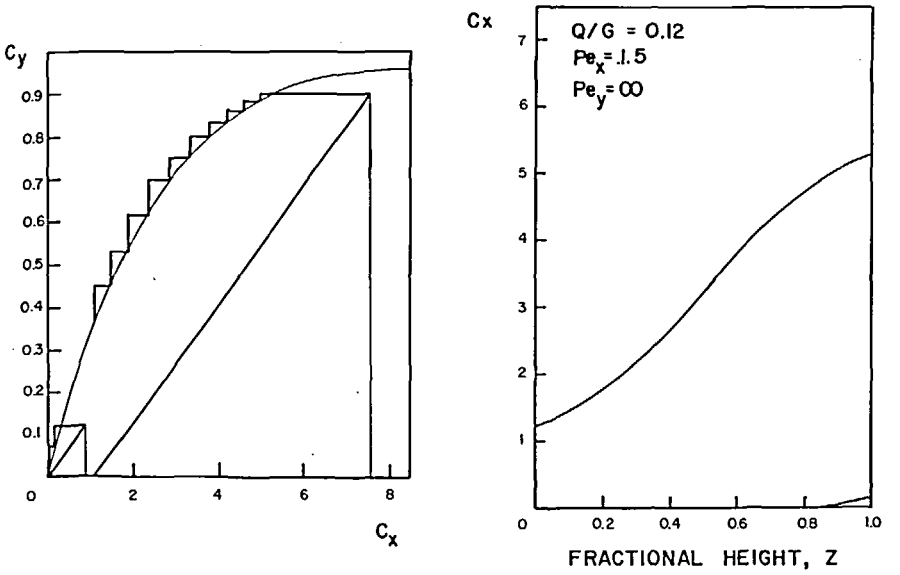

FIGURE 18
Graphical construction and resulting calculated copper removals and concentration profiles for combined bubble and foam fractionation. Case 1: Surfactant concentration constant axially (construction not shown); Case 2: Surfactant added to main feed and stripped in section below feed.

the flows do not change, but two different feed concentrations of copper--7.5 and 0.8 ppm--are considered. The smaller feed concentration gives the greater percent removal and also gives a lower ratio of C_x at z=0 to C_{in}.

Figure 20 shows the results of experiments made with the same 6.95-cm diameter column. The column was operated with a main liquid feed flow of 5.7 cm^3/sec containing 0.080 millimoles/liter of Neodol 25-3A and various concentrations of copper, entering 5.2 feet above the bottom. A second liquid feed with a flow of 0.19 cm^3/sec and containing 2.3 millimoles/liter of Neodol 25-3A entered one foot above the bottom. The volumetric flow

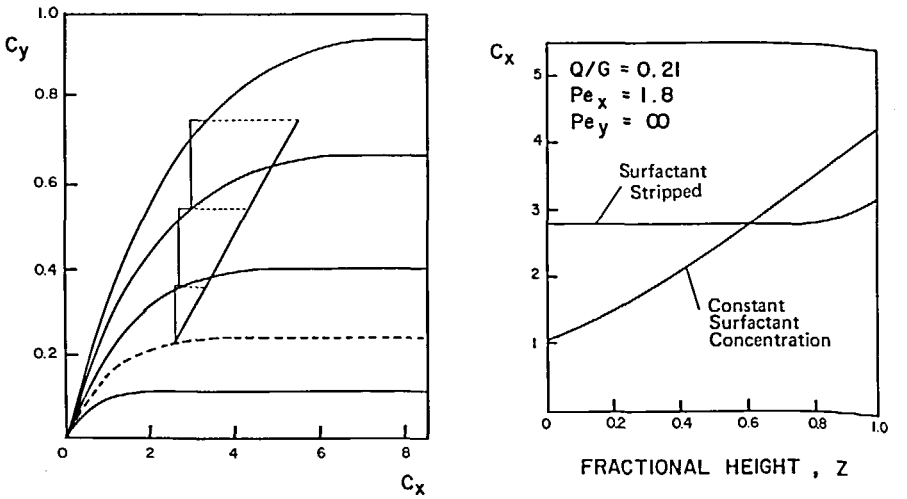

FIGURE 19
Graphical construction and resulting calculated copper removals and concentration profiles for combined bubble and foam fractionation with surfactant concentration axially constant and with different copper concentrations in feed.

ratio was G/L=5.53. In fig. 20 concentrations are plotted vs the distance above the bottom of the column. The Neodol concentration is indicated by circles and the dashed curve. Notice that the lower-level surfactant feed serves to keep the surfactant concentration relatively high. Note also that a greater length of column below the lower feed would be required for effective stripping of Neodol from the raffinate. The surfactant concentration profiles were essentially the same for all measurements reported in fig. 20, since the surface activity of Neodol 25-3A was found not to be affected appreciably by changes in copper concentration.

The three solid curves in fig. 20 are measured concentration profiles for three different feed concentrations of copper; these feed concentrations are shown as solid points beside the right-hand axis. Notice that the

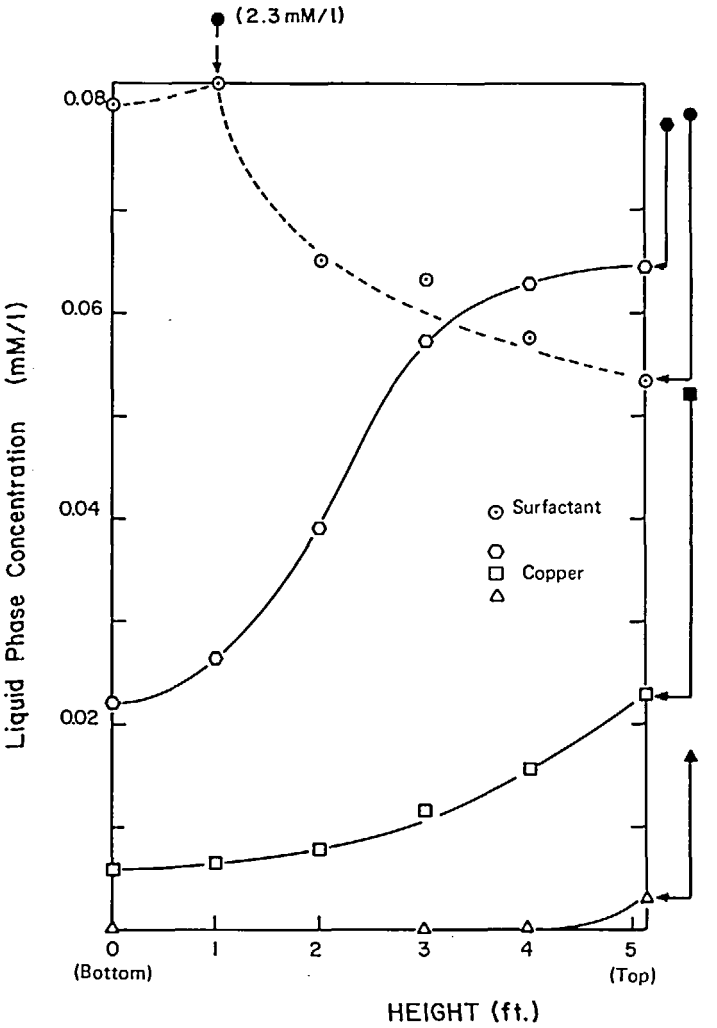

FIGURE 20
Measured axial concentration profiles for Neodol 25-3A and copper during combined bubble and foam fractionation in 6.95-cm diameter column. A small, concentrated surfactant feed is introduced 1 ft. above the bottom, and the main, copper-bearing feed is introduced 5.2 ft. above the bottom.

trend of profile shape from high to low copper concentrations in the feed follows the predictions from the construction shown in fig. 19. Greater percent-wise removals are found for lower feed concentrations, and the ratio of C_x at z=0 to C_{in} is less for lower feed concentrations. This behavior with respect to feed concentration was also found in fig. 19.

Column Alignment

It has been found[64] that the degree of axial dispersion and the resultant separations and axial concentration profiles obtained in a column are very sensitive to slight departures from perfect vertical alignment, even for variations in alignment as small as 1°. Thus, if a column is designed to take advantage of a substantial amount of bubble fractionation within the liquid pool, it is important that the alignment of the column with respect to the vertical be true.

Scale-Up

Valdes-Krieg, et al.[41] report results obtained with a column 1 ft. x 1 ft. square in cross-section and 6 ft. high, processing seawater and related solutions for removal of surfactant. In fig. 4 of that paper, it is shown that flow conditions giving smooth operation could in some cases give a substantial enhancement of separation due to bubble fractionation in the liquid pool. However, as the column cross-section dimension increases, E_x becomes larger; hence Pe_x becomes lower and the separation axially along the liquid becomes less.

It appears that for large-scale operation there is a choice to be made between single-stage, well-mixed-pool operation, on the one hand, and some form of construction that preserves a high length-to-diameter ratio in the liquid phase, on the other hand. The latter case can give a substantial concentration gradient and

thereby an improved separation, but at the expense of a more elaborate construction.

Acknowledgement

The work presented from our own laboratory was supported financially by grants from the Office of Saline Water (U.S. Dept. of the Interior) and from Kennecott Copper Corporation (Ledgemont Laboratory). One of the authors (E.V.K.) also received financial support from CONACYT, Mexico.

References

[1] Environmental Protection Agency (U.S.), Report No. EPA-902/9-74-001, New York (1974).

[2] E. Rubin & E.L. Gaden, in "New Chemical Engineering Separation Techniques", H.M. Schoen, ed., Interscience, NY, 1962.

[3] R. Lemlich, ed., "Adsorptive Bubble Separation Techniques", Academic Press, NY, 1972.

[4] R. Lemlich, "The Adsorptive Bubble Separation Techniques" in "Traces of Heavy Metals in Water: Removal Processes and Monitoring", Environmental Protection Agency, EPA-902/9-74-001, 1974.

[5] P. Somasundaran, Separation & Purification Methods, 1, 1 (1972).

[6] R.B. Grieves, Chem. Eng. Jour., 9, 93 (1975).

[7] B.L. Karger, R.B. Grieves, R. Lemlich, A.J. Rubin & F. Sebba, Sep. Sci., 2, 401 (1967).

[8] R.A. Leonard & R. Lemlich, AIChE Jour., 11, 18 (1965).

[9] P.A. Haas & H.F. Johnson, AIChE Jour., 11, 319 (1965).

[10]P.A. Haas & H.F. Johnson, Ind. Eng. Chem. Fund., 6, 225 (1967).
[11]J.J. Bikerman, "Foams", Springer, NY, 1973.
[12]R. Lemlich & E. Lavi, Science 134, 191 (1961).
[13]P.F. Wace & D.L. Banfield, Chem. & Proc. Eng., 47, 71 (1966).
[14]P.A. Haas, Report No. ORNL-3527, Oak Ridge Natl. Lab., Oak Ridge, TN, 1965.
[15]G.H. Robertson & T. Vermeulen, "Foam Fractionation of Rare Earth Elements", Univ. of Calif. Lawrence Radiation Lab., UCRL 19525 (1969).
[16]R.B. Grieves & G.A. Ettelt, AIChE Jour., 13, 1167 (1967).
[17]F. Sebba, Nature, 184, 1062 (1959).
[18]F. Sebba, "Ion Flotation", American Elsevier, NY, 1962.
[36]J.T. Davies, Proc. 2nd Int. Congr. Surf. Activity, 1, 426 (1958).
[37]R.M. Reed & H.V. Tartar, J. Amer. Chem. Soc., 58, 323 (1936).
[38]E. Valdes-Krieg, Ph.D. Dissertation in Chemical Engineering, Univ. of Calif., Berkeley, 1975.
[39]A.F.H. Ward & L. Tordai, Nature, 158, 416 (1946).
[40]R.B. Grieves & D. Bhattacharyya, J. Water Poll. Control Federation, 37, 7 (1965).
[41]E. Valdes-Krieg, C.J. King & H.H. Sephton, Desalination, 16, 39 (1975).
[42]R. Matuura, H. Kimizuka & A. Matsubara, Bull. Chem. Soc. Japan, 34, 1512 (1961).
[43]M.K. Muramatsu, K. Tajima, M. Iwahashi & K. Nukina, J. Coll. & Int. Sci., 43, 499 (1973).
[44]C.A. Brunner & R. Lemlich, Ind. Eng. Chem. Fund., 2, 297 (1963).
[45]E. Valdes-Krieg, C.J. King & H.H. Sephton, AIChE Symp. Ser., 71, No. 150, 46 (1975).

[46]W.D. Deckwer, U. Grasser, H. Langemann & Y. Serpemen, Chem. Eng. Sci., 28, 1223 (1973).
[47]C. Walling, E.E. Ruff & J.L. Thornton, J. Phys. Chem., 61, 486 (1957).
[48]R. Lemlich, Chem. Eng. Sci., 23, 932 (1968).
[49]J. Jorné & E. Rubin, Separ. Sci., 4, 313 (1969).
[50]D.J. Shaw, "Introduction to Colloid and Surface Chemistry", Butterworths, London, 1966.
[51]F. Helfferich, "Ion Exchange", Wiley, NY, 1962.
[52]T. Vermeulen, G. Klein & N.K. Hiester, in "Chemical Engineers' Handbook", 5th ed., R.H. Perry & C.H. Chilton, eds., McGraw-Hill, NY, 1973.
[53]W.L. Dick & F.D. Talbot, Ind. Eng. Chem. Fund., 10, 309 (1971).
[53]R.C.H. Huang & F.D. Talbot, Can. J. Chem. Eng., 51,
[19]A.M. Gaudin, "Flotation", McGraw-Hill, NY, 1957.
[20]D.W. Fuerstenau, ed., "Froth Flotation--50th Anniversary Volume", AIME, NY, 1962.
[21]D.W. Fuerstenau & T.W. Healy, in "Adsorptive Bubble Separation Techniques", R. Lemlich, ed., Academic Press, NY, 1972.
[22]C. Jacobelli-Turi, A. Margani & M. Palmera, Ric. Sci., 36, 198 (1966).
[23]A.J. Rubin, J.D. Johnson & J.C. Lamb, Ind. Eng. Chem. Proc. Des. & Devel., 5, 368 (1966).
[24]C.P. Beitelshees, C.J. King & H.H. Sephton, paper pres. at ACS mtg., San Francisco, CA, August 1976. in "Recent Developments in Separation Science", N.N. Li, ed., vol. 5-6, CRC Press, Cleveland, 1977.
[25]A.J. Rubin & S.F. Erickson, Water Resources, 4, 98 (1971).
[26]Y.S. Kim & H. Zeitlin, Sep. Sci. 6, 505 (1971).
[27]R. Lemlich & D.O. Harper, Ind. Eng. Chem. Proc. Des. & Devel., 4, 13 (1965).

[28]R. Lemlich & D.O. Harper, AIChE Jour., 12, 1220 (1966).
[29]K.D. Cannon & R. Lemlich, Chem. Eng. Prog. Symp. Ser., 68, No. 124, 180 (1972).
[30]S. Bruin, J.E. Hudson & A.I. Morgan, Jr., Ind. Eng. Chem., Fund., 11, 175 (1972).
[31]R.W. Schnepf, E.L. Gaden, Jr., E.Y. Mirocznik & E. Schonfeld, Chem. Eng. Prog., 55(5), 42 (1959).
[32]J.W. Gibbs, "Collected Works", Vol. 1, Longmans Green, NY, 1928.
[33]J.T. Davies & E.K. Rideal, "Interfacial Phenomena", Academic Press, NY, 1961.
[34]I.J. Lin & P. Somasundaran, J. Coll. Int. Sci., 37(4), 731 (1971).
[35]A.W. Adamson, "Physical Chemistry of Surfaces", 2nd edition, Wiley Interscience, NY, 1967.
709 (1973).
[55]A.J. Rubin & J.C. Johnston, Anal. Chem., 39, 298 (1967).
[56]J. Arod, in "Adsorptive Bubble Separation Techniques", R. Lemlich, ed., Academic Press, NY, 1972.
[57]I.L. Jashnani & R. Lemlich, Ind. Eng. Chem. Proc. Des. Dev., 12, 312 (1973).
[58]T. Miyauchi & T. Vermeulen, Ind. Eng. Chem. Fund., 2, 113 (1963).
[59]K.D. Cannon & R. Lemlich, Chem. Eng. Prog. Symp. Ser., 68, No. 124, 180 (1972).
[60]B.T. Kwon & K.L. Wang, Sep Sci., 6, 537 (1971).
[61]V. Rod, Brit. Chem. Eng., 9, 300 (1964).
[62]Office of Saline Water, Disposal of the Effluents from Desalination Plants: The Effects of Copper Content, Heat and Salinity, U.S. Govt. Printing Office, Wash., D.C. (1969).

[63]E. Valdes-Krieg, C.J. King & H.H. Sephton, "Foam and Bubble Fractionation for the Removal of Trace Metal Ions from Water", in U.S. Environmental Protection Agency Report No. EPA-902/9-74-001 (1974).

[64]E. Valdes-Krieg, C.J. King & H.H. Sephton, AIChE Jour., 21, 400 (1975).